arXiv:quant-ph/0609071v2 14 Feb 2007

Optical state engineering, quantum communication, and robustness of entanglement promiscuity in three-mode Gaussian states

Gerardo Adesso[1,2,3], **Alessio Serafini**[4,5] **and Fabrizio Illuminati**[1]

[1]Dipartimento di Fisica "E. R. Caianiello", Università degli Studi di Salerno; CNR-Coherentia, Gruppo di Salerno; and INFN Sezione di Napoli-Gruppo Collegato di Salerno; Via S. Allende, 84081 Baronissi (SA), Italy
[2]Centre for Quantum Computation, DAMTP, Centre for Mathematical Sciences, University of Cambridge, Wilberforce Road, Cambridge CB3 0WA, United Kingdom
[3]Dipartimento di Fisica dell'Università "La Sapienza" and Consorzio Nazionale Interuniversitario per le Scienze Fisiche della Materia, Roma, 00185 Italy
[4]Institute for Mathematical Sciences, Imperial College London, 53 Prince's Gate, SW7 2PE, United Kingdom; and QOLS, The Blackett Laboratory, Imperial College London, Prince Consort Road, SW7 2BW, United Kingdom
[5]Department of Physics & Astronomy, University College London, Gower Street, London WC1E 6BT, United Kingdom
E-mail: gerardo@sa.infn.it, serale@imperial.ac.uk, illuminati@sa.infn.it

Abstract. We present a novel, detailed study on the usefulness of three-mode Gaussian states states for realistic processing of continuous-variable quantum information, with a particular emphasis on the possibilities opened up by their genuine tripartite entanglement. We describe practical schemes to engineer several classes of pure and mixed three-mode states that stand out for their informational and/or entanglement properties. In particular, we introduce a simple procedure – based on passive optical elements – to produce pure three-mode Gaussian states with *arbitrary* entanglement structure (upon availability of an initial two-mode squeezed state). We analyze in depth the properties of distributed entanglement and the origin of its sharing structure, showing that the promiscuity of entanglement sharing is a feature peculiar to symmetric Gaussian states that survives even in the presence of significant degrees of mixedness and decoherence. Next, we discuss the suitability of the considered tripartite entangled states to the implementation of quantum information and communication protocols with continuous variables. This will lead to a feasible experimental proposal to test the promiscuous sharing of continuous-variable tripartite entanglement, in terms of the optimal fidelity of teleportation networks with Gaussian resources. We finally focus on the application of three-mode states to symmetric and asymmetric telecloning, and single out the structural properties of the optimal Gaussian resources for the latter protocol in different settings. Our analysis aims to lay the basis for a practical quantum communication with continuous variables beyond the bipartite scenario.

PACS numbers: 03.67.Mn, 03.67.Hk, 03.65.Ud

Contents

1. Introduction

The study of *multipartite* entanglement in Gaussian states of continuous variable systems has lately received much attention, both in view of their interest as a theoretical testground and because of their versatility towards the effective implementation of communication protocols. Nevertheless, a complete understanding of the general features of multipartite quantum correlations and of their (often controversial) operational interpretation still appears to be far from accomplished.

For the basic instance of three-mode Gaussian states, a qualitative classification of multipartite entanglement has been introduced [1], while more recently a consistent way to quantify such a multipartite entanglement has been presented, with the definition of the "residual (Gaussian) contangle" [2]. It has also been shown that pure, symmetric three-mode Gaussian states exhibit a *promiscuous* sharing of quantum correlations (where bipartite and genuine multipartite entanglement are not mutually exclusive but rather reciprocally enhanced) [3, 2]. However, several important aspects related to the complex sharing structure of quantum correlations between the three parties await for further inspection and clarification.

In this respect, the purpose of this paper is threefold. Firstly, it investigates the origin of the promiscuous entanglement sharing and shows that it is crucially related to the global symmetry of the states (as its signature is still present in mixed, symmetric, while it is lost in pure, asymmetric states). Secondly, it presents practical strategies to engineer three-mode Gaussian entangled states, which may have a remarkable experimental impact towards the practical realization of optimal resources for specific multipartite communication tasks. Thirdly, it aims at providing the residual contangle and its properties with an operational interpretation by addressing its relationship with the figures of merits of optimized communication protocols (teleportation networks and telecloning). As we will see, these two objectives are intimately intertwined, as they both concern the characterization of the structure of multipartite entanglement and of its sharing properties.

The article opens with a brief review of the basic properties of three-mode Gaussian states and of their entanglement (Sec. 2). We then proceed to investigate the sharing of quantum correlations in asymmetric, mixed three-mode states, introducing a paradigmatic class of states (which will be dubbed "basset hound" states) and showing that symmetric mixed states still feature a promiscuous entanglement sharing, whereas pure asymmetric states lose such a peculiarity (Sec. 3). In Sec. 4, we describe a novel, 'economical' (in a well-defined sense) strategy to build pure three-mode Gaussian states with any, arbitrary entanglement structure; furthermore, we present guidelines for the optical generation of classes of pure and noisy three-mode Gaussian with relevant entanglement properties. Sec. 5 introduces the second part of the paper, devoted to communication protocols. In Sec. 6 we review and discuss the equivalence between the optimal fidelities of three-party teleportation networks and Gaussian residual contangle in symmetric pure resources, proposing a direct experimental test of the promiscuous sharing; the demise of the optimal fidelity under thermal decoherence of the three-mode resource is also exactly studied and pure symmetric states are shown to be the most robust (in the specific sense of optimally preserving the maximal fidelity under decoherence). In Sec. 7 we focus on symmetric and asymmetric telecloning, showing that the operational interpretation of entanglement measures in terms of teleportation fidelity breaks down for asymmetric states and determining several instances of three-mode states acting as optimal (under various constraints) resources for such communication protocols. Sec. 8 concludes the paper, finalizing the line of work undertaken in Ref. [2] and completed in the present article.

2. Three-mode Gaussian states: structural and entanglement properties

We consider a continuous variable (CV) system consisting of N bosonic modes, associated to an infinite-dimensional Hilbert space $\mathcal{H}$ and described by the vector $\hat{X} = \{\hat{x}_1, \hat{p}_1, \ldots, \hat{x}_N, \hat{p}_N\}$ of the field quadrature operators, whose canonical commutation relations can be expressed in matrix form: $[\hat{X}_i, \hat{X}_j] = 2i\Omega_{ij}$, with the symplectic form $\Omega = \oplus_{i=1}^{n}\omega$ and $\omega = \delta_{ij-1} - \delta_{ij+1}$, $i, j = 1, 2$.

Quantum states of paramount importance in CV systems are the so-called Gaussian states, *i.e.* states with Gaussian characteristic functions and quasi-probability distributions [4, 5, 6, 7]. The interest in this special class of states (which includes vacua, coherent, squeezed, thermal, and squeezed-thermal states of the electromagnetic field) stems from the feasibility to produce and control them with linear optical elements, and from the increasing number of efficient proposals and successful implementations of quantum information and communication protocols involving multimode Gaussian states. For a review of the basic properties of Gaussian states and their structural and entanglement characterization, see *e.g.* Ref. [7]. A more concise (and closely related to the context of this paper) background is provided in Ref. [2], which is focused on three-mode states and contains a quite general introduction to phase-space formalism and symplectic operations (making use of the same notation adopted here). In this section, we limit ourselves to define the relevant notation and recall some useful results.

Neglecting first moments (which can be arbitrarily adjusted by local unitaries), one can completely characterize a Gaussian state by the real, symmetric covariance matrix (CM) $\boldsymbol{\sigma}$, whose entries are $\sigma_{ij} = 1/2\langle\{\hat{X}_i, \hat{X}_j\}\rangle - \langle\hat{X}_i\rangle\langle\hat{X}_j\rangle$. Throughout the paper $\boldsymbol{\sigma}$ will be used indifferently to indicate the CM of a Gaussian state or the state itself. The CM $\boldsymbol{\sigma}$ must fulfill the Robertson-Schrödinger uncertainty relation $\boldsymbol{\sigma} + i\Omega \geq 0$ [8].

For future convenience, let us write down the CM $\boldsymbol{\sigma}$ of a 3-mode Gaussian state in terms of two by two submatrices as

$$\boldsymbol{\sigma} = \begin{pmatrix} \boldsymbol{\sigma}_1 & \boldsymbol{\varepsilon}_{12} & \boldsymbol{\varepsilon}_{13} \\ \boldsymbol{\varepsilon}_{12}^{\mathsf{T}} & \boldsymbol{\sigma}_2 & \boldsymbol{\varepsilon}_{23} \\ \boldsymbol{\varepsilon}_{13}^{\mathsf{T}} & \boldsymbol{\varepsilon}_{23}^{\mathsf{T}} & \boldsymbol{\sigma}_3 \end{pmatrix} . \tag{1}$$

In what follows, we will refer to three-mode Gaussian states endowed with symmetries under mode exchange as "bisymmetric" (invariant under the permutation of a specific pair of modes) and "fully symmetric" states (invariant under the permutation of any pair of modes). In terms of the 2×2 blocks of Eq. (1), the CM of three-mode bisymmetric states is defined by $\boldsymbol{\sigma}_j = \boldsymbol{\sigma}_k$ and $\boldsymbol{\varepsilon}_{jl} = \boldsymbol{\varepsilon}_{kl}$ for indexes $j \neq k \neq l$ with values between 1 and 3. Clearly, fully symmetric states have

$$\boldsymbol{\alpha} \equiv \boldsymbol{\sigma}_1 = \boldsymbol{\sigma}_2 = \boldsymbol{\sigma}_3 \quad \text{and} \quad \boldsymbol{\zeta} \equiv \boldsymbol{\varepsilon}_{12} = \boldsymbol{\varepsilon}_{13} = \boldsymbol{\varepsilon}_{23} \, . \tag{2}$$

The entanglement of bisymmetric states can be concentrated in two modes by local unitary operations [9, 10].‡ In general, for $(M + N)$-mode states, bisymmetric states are defined as invariant under the exchange of any two modes within the subsystems of M and N modes.

2.1. Separability properties

The positivity of the partially transposed CM $\tilde{\boldsymbol{\sigma}}$ has been proven to be necessary and sufficient for the separability of $(1 + N)$-mode and bisymmetric $(M + N)$-mode Gaussian states [11, 12, 13, 9], providing a clearcut qualitative characterization of the entanglement of such

‡ A pictorial description of such unitary-localization procedure is provided in the following (see Fig. 2).

states (PPT criterion). An ensuing computable measure of CV entanglement is the *logarithmic negativity* [14] $E_{\mathcal{N}} \equiv \ln \|\tilde{\varrho}\|_1$, where $\|\cdot\|_1$ denotes the trace norm, which constitutes an upper bound to the *distillable entanglement* of the state ϱ. For Gaussian states, it can be computed in terms of the symplectic spectrum $\tilde{\nu}_i$ of the partially transposed CM $\tilde{\boldsymbol{\sigma}}$ [2]:

$$E_{\mathcal{N}} = \max\left\{0, -\sum\nolimits_{i:\tilde{\nu}_i<1} \ln \tilde{\nu}_i\right\} . \tag{3}$$

A complete *qualitative* characterization of the entanglement of three-mode Gaussian state has been obtained in [1], where five different instances have been classified according to their separability properties under different bipartitions. Let us also recall that, from a more practically-oriented viewpoint, efficient criteria to detect multipartite entanglement from the knowledge of the second moments have been developed in [15]. Moreover, another effective way of testing the presence of bipartite and/or genuine tripartite entanglement in Gaussian states is through *entanglement witnesses*, based on linear and nonlinear functionals of the CM [16].

As for the *quantification* of the tripartite entanglement of Gaussian states, it has been shown in [3, 17] that, assuming the *'contangle'* $E_\tau^{j|k}$ as an entanglement measure (formally defined as the convex roof of the squared logarithmic negativity, here the notation $j|k$ refers to some pair of subsystems), a 'monogamy' inequality [18] analogous to the finite dimensional one [19, 20] holds. For three modes, the inequality reads: $E_\tau^{j|(kl)} - E_\tau^{j|k} - E_\tau^{j|l} \geq 0$, where j, k, l label the three modes and can be permuted at will. One can also define the *Gaussian contangle* $G_\tau^{j|k}$, where the convex roof is restricted to Gaussian decompositions. Clearly, the Gaussian contangle is in general easier to handle analytically than the contangle; it fulfills the monogamy inequality as well. The monogamy constraints suggest proper quantifiers of genuine tripartite entanglement. In particular, the minimum *residual contangle* E_τ^{res} [3] is defined as

$$E_\tau^{res} \equiv \min_{(i,j,k)} \left[E_\tau^{i|(jk)} - E_\tau^{i|j} - E_\tau^{i|k}\right] , \tag{4}$$

where (i, j, k) denotes all the permutations of the three mode indexes. Likewise, the minimum residual Gaussian contangle G_τ^{res}, compactly referred to as *arravogliament* (or "arravojament") [3, 2], reads

$$G_\tau^{res} \equiv G_\tau^{i|j|k} \equiv \min_{(i,j,k)} \left[G_\tau^{i|(jk)} - G_\tau^{i|j} - G_\tau^{i|k}\right] . \tag{5}$$

Such a measure is monotonic under Gaussian local operations and classical communication [3] and will be adopted to quantify the genuine tripartite entanglement of three-mode Gaussian states. The operational status of this measure will be discussed in the final part of the paper, in terms of teleportation fidelities.

As demonstrated in Ref. [2], the three local symplectic invariants $\mathrm{Det}\,\boldsymbol{\sigma}_1$, $\mathrm{Det}\,\boldsymbol{\sigma}_2$ and $\mathrm{Det}\,\boldsymbol{\sigma}_3$ (strictly related to the local mixednesses of the state [21]) fully determine the entanglement of any possible bipartition of a pure three-mode Gaussian state with CM $\boldsymbol{\sigma}$, and also the genuine tripartite entanglement contained in the state [3]. Moreover, defining $a_j \equiv \sqrt{\mathrm{Det}\,\boldsymbol{\sigma}_j}$ for $j = 1, \ldots, 3$ one has that the three single-mode mixednesses are constrained by the following 'triangle' entropic inequality (see [2] for a detailed proof)

$$|a_i - a_j| + 1 \leq a_k \leq a_i + a_j - 1 . \tag{6}$$

Remarkably, Inequality (6) (together with the conditions $a_l \geq 0\ \forall l$) fully characterizes the local symplectic eigenvalues of the CM of three-mode pure Gaussian states, thus providing a complete characterization of the entanglement of such states. In fact, the CM of Eq. (1) can be put in a *standard form* completely parametrized by the three local mixednesses, with

$\boldsymbol{\sigma}_i = \mathrm{diag}\{a_i,\, a_i\}$ and the blocks $\boldsymbol{\varepsilon}_{ij}$ diagonal as well, with elements only functions of the $\{a_i\}$'s [2].

3. Promiscuous entanglement sharing versus noise and asymmetry

In Ref. [3], as a direct application of the monogamy constraint on the distribution of tripartite quantum correlations, the entanglement sharing structure of three-mode Gaussian states has been investigated. In particular, it has been demonstrated that pure, fully symmetric (*i.e.* with $\mathrm{Det}\,\boldsymbol{\sigma}_1 = \mathrm{Det}\,\boldsymbol{\sigma}_2 = \mathrm{Det}\,\boldsymbol{\sigma}_3 \equiv a$ in Eq. (1)) Gaussian states exist which are maximally three-way entangled and, at the same time, possess the maximum possible entanglement between any pair of modes in the corresponding two-mode reduced states. Those states, known as CV finite-squeezing GHZ/W states, are thus said to exhibit a *promiscuous* entanglement sharing [3, 2]. The notion of "promiscuity" basically means that bipartite and genuine multipartite (in this case tripartite) entanglement are increasing functions of each other, and the genuine tripartite entanglement is enhanced by the simultaneous presence of the bipartite one, while typically in low-dimensional systems like qubits only the opposite behaviour is compatible with monogamy [19, 22]. The promiscuity of entanglement in three-mode GHZ/W states is, however, *partial*§. Namely they exhibit, with increasing squeezing, an unlimited tripartite entanglement given by [2]

$$G_\tau^{res}(\boldsymbol{\sigma}^{\mathrm{GHZ}/W}) = \mathrm{arcsinh}^2\Big[\sqrt{a^2-1}\Big] - \frac{1}{2}\ln^2\left[\frac{3a^2-1-\sqrt{9a^4-10a^2+1}}{2}\right], \quad (7)$$

and thus diverging in the limit $a \to \infty$. At the same time, they also possess a nonzero, accordingly increasing bipartite entanglement between any two modes, which nevertheless stays finite even for infinite squeezing. Precisely, from Eq. (7), it saturates to the value

$$G_\tau^{i|j}(\boldsymbol{\sigma}^{\mathrm{GHZ}/W},\, a\to\infty) = \frac{\ln^2 3}{4} \approx 0.3\,. \quad (8)$$

We will see later on how this promiscuous distribution of entanglement can be demonstrated experimentally in terms of CV teleportation experiments. Prior to that, it is natural to question whether *all* three-mode Gaussian states are expected to exhibit a promiscuous entanglement sharing. So far, such a question has not yet been addressed. We shall therefore investigate the robustness of promiscuity against the lack of each of the two defining properties of GHZ/W states: full symmetry, and global purity. We will specifically find that promiscuity survives under mixedness, but is in general lost if the complete permutation-invariance is relaxed.

*3.1. Promiscuity versus mixedness: Entanglement distribution in noisy GHZ/*W *states*

We consider here the noisy version of the three-mode GHZ/W states, which are a family of mixed Gaussian fully symmetric states, also called three-mode squeezed thermal states [24]. They result in general from the dissipative evolution of pure GHZ/W states in proper Gaussian noisy channels [2]. Let us mention that various properties of noisy three-mode Gaussian states have already been addressed, mainly regarding their effectiveness in the implementation of CV protocols [25, 26]. However, here we focus on the properties of genuine multipartite entanglement of such states, which have not been considered previously. This analysis will

§ It can be in fact shown that in Gaussian states of CV systems with more than three modes, entanglement can be distributed in an *infinitely* promiscuous way [23].

allow us to go beyond the set of pure states, thus gaining deeper insight into the role played by realistic quantum noise in the sharing and characterization of tripartite entanglement.

Noisy GHZ/W states are described by a fully symmetric CM $\boldsymbol{\sigma}_s^{th}$ of the form (2), with $\boldsymbol{\alpha} = a\mathbb{1}_2$ and $\boldsymbol{\zeta} = \mathrm{diag}\{e^+,\, e^-\}$, where

$$e^{\pm} = \frac{a^2 - n^2 \pm \sqrt{(a^2 - n^2)\,(9a^2 - n^2)}}{4a}\,, \tag{9}$$

where $a \geq n$ to ensure the physicality of the state. These states are thus completely determined by the local purity $\mu_l = a^{-1}$ and by the global purity $\mu = n^{-3}$.‖ For ease of notation, let us replace the parameter a with the "'squeezing parameter" s, defined by $3as = n\sqrt{2s^4 + 5s^2 + 2}$ (whose physical significance will become clear once the experimental generation of GHZ/W will be described in Sec. 4.2.1). Noisy GHZ/W states reduce to pure GHZ/W states (*i.e.* three-mode squeezed *vacuum* states) for $n = 1$.

3.1.1. Separability properties Depending on the defining parameters s and n, noisy GHZ/W states can belong to three different separability classes according to the classification of Ref. [1]. Namely, as explicitly computed in Ref. [24], we have in our notation

$$s > \frac{\sqrt{9n^4 - 2n^2 + 9 + 3\,(n^2 - 1)\,\sqrt{9n^4 + 14n^2 + 9}}}{4n} \qquad \Rightarrow \textit{Class 1;} \tag{10}$$

$$n < s \leq \frac{\sqrt{9n^4 - 2n^2 + 9 + 3\,(n^2 - 1)\,\sqrt{9n^4 + 14n^2 + 9}}}{4n} \Rightarrow \textit{Class 4;} \tag{11}$$

$$s \leq n \qquad \Rightarrow \textit{Class 5.} \tag{12}$$

States which fulfill Ineq. (10) are fully inseparable (Class 1, encoding genuine tripartite entanglement), while states that violate it have positive partial transposition with respect to all bipartitions. However, in this case PPTness does not imply separability. In fact, in the range defined by Ineq. (11), noisy GHZ/W states are three-mode biseparable (Class 4), that is they exhibit tripartite *bound entanglement*. This can be verified by showing, using the methods of Ref. [1], that such states cannot be written as a convex combination of separable states. Finally, noisy GHZ/W states that fulfill Ineq. (12) are fully separable (Class 5), containing no entanglement at all.

The tripartite residual Gaussian contangle of Eq. (5), which is nonzero only in the fully inseparable region, can be explicitly computed. In particular, the 1×2 Gaussian contangle $G_\tau^{i|(jk)}$ is obtained by exploiting the *unitary localizability* of entanglement in symmetric Gaussian states [9]. Namely, if one lets modes 2 and 3 interfere at a 50:50 beam-splitter, this operation (local unitary with respect to the imposed $1|(23)$ bipartition) decouples the transformed mode $3'$ (more details will be given later, see Fig. 2). Moreover, one finds that the resulting equivalent two-mode state of modes 1 and $2'$ is symmetric, and so the bipartite contangle between mode 1 and the block of modes (23), equal to the bipartite contangle between modes 1 and $2'$, coincides with the squared logarithmic negativity [3]. As for the two-mode Gaussian contangles $G_\tau^{1|2} = G_\tau^{1|3}$, the same result holds, as the reduced states are symmetric. Finally one gets, in the range defined by Ineq. (10), a tripartite entanglement given by

$$G_\tau^{res}(\boldsymbol{\sigma}_s^{th}) = \frac{1}{4}\ln^2\left\{\frac{n^2\left[4s^4 + s^2 + 4 - 2\left(s^2 - 1\right)\sqrt{4s^4 + 10s^2 + 4}\right]}{9s^2}\right\}$$

‖ The "purity" μ fo a quantum state ϱ is given by $\mathrm{Tr}\,(\varrho^2)$. For a Gaussian state ϱ with CM $\boldsymbol{\sigma}$ one has $\mu = 1/\sqrt{\mathrm{Det}\,\boldsymbol{\sigma}}$ [21].

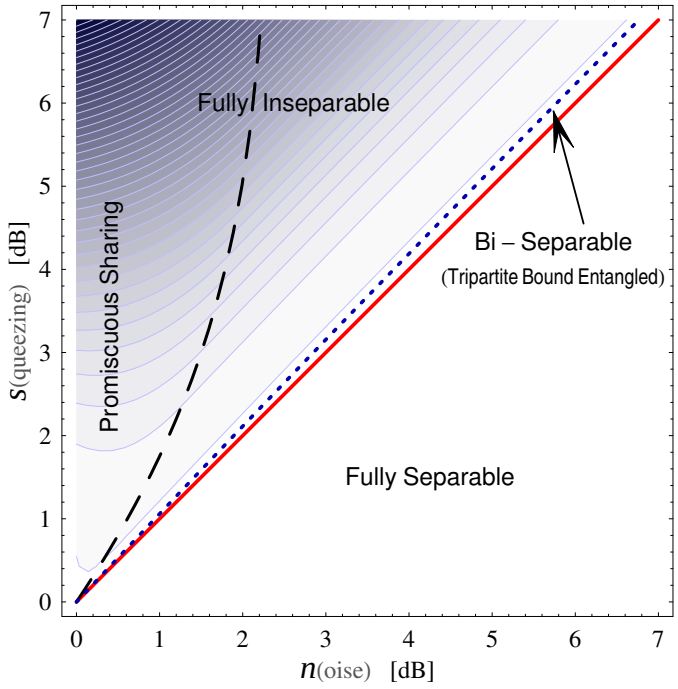

Figure 1. Summary of separability and entanglement properties of three-mode squeezed thermal states, or noisy GHZ/W states, in the space of the two parameters n and s. The separability is classified according to the scheme of Ref. [1]. Above the dotted line the states are fully inseparable (Class 1); below the solid line they are fully separable (Class 5). In the narrow intermediate region, noisy GHZ/W states are three-mode biseparable (Class 4), *i.e.* they exhibit tripartite bound entanglement. The relations defining the boundaries for the different regions are given in Eqs. (10–12). In the fully inseparable region, the residual (Gaussian) contangle Eq. (13) is depicted as a contour plot, growing with increasing darkness from $G_\tau^{res} = 0$ (along the dotted line) to $G_\tau^{res} \approx 1.9$ (at $n = 0$ dB, $s = 7$ dB). On the left side of the dashed line, whose expression is given by Eq. (15), not only genuine tripartite entanglement is present, but also each reduced two-mode bipartition is entangled. In this region, G_τ^{res} is strictly larger than in the region where the two-mode reductions are separable. This evidences the *promiscuous* sharing structure of multipartite CV entanglement in symmetric, even mixed, three-mode Gaussian states.

$$- 2 \left[\max \left\{ 0, - \ln \left(\frac{n\sqrt{s^2+2}}{\sqrt{3}s} \right) \right\} \right]^2 , \tag{13}$$

and $G_\tau^{res}(\boldsymbol{\sigma}_s^{th}) = 0$ when Ineq. (10) is violated. For noisy GHZ/W states, the residual Gaussian contangle Eq. (13) is still equal to the true one Eq. (4) (like in the special instance of pure GHZ/W states), thanks to the symmetry of the two-mode reductions, and of the unitarily transformed state of modes 1 and $2'$.

3.1.2. Sharing structure The second term in Eq. (13) embodies the sum of the couplewise entanglement in the $1|2$ and $1|3$ reduced bipartitions. Therefore, if its presence enhances the value of the tripartite residual contangle (as compared to what happens if it vanishes), then one can infer that entanglement sharing is 'promiscuous' in the (mixed) three-mode squeezed thermal Gaussian states as well ('noisy GHZ/W' states). And this is exactly the case, as shown in the contour plot of Fig. 1, where the separability and entanglement properties of

noisy GHZ/W states are summarized, as functions of the parameters n and s expressed in decibels.¶ Explicitly, one finds that for

$$n \geq \sqrt{3}\,, \tag{14}$$

corresponding to ≈ 2.386 dB of noise, the entanglement sharing can never be promiscuous, as the reduced two-mode entanglement is zero for any (even arbitrarily large) squeezing s. Otherwise, applying PPT criterion to any two-mode reduction one finds that for sufficiently high squeezing s bipartite entanglement is also present in any two-mode reduction, namely

$$n < \sqrt{3} \quad \text{and} \quad s > \frac{\sqrt{2}n}{\sqrt{3-n^2}} \quad \Rightarrow \quad \textit{promiscuous} \text{ sharing}\,. \tag{15}$$

Evaluation of Eq. (13), as shown in Fig. 1, clearly demonstrates that the genuine tripartite entanglement increases with increasing bipartite entanglement in any two-mode reduction, unambiguously confirming that CV quantum correlations distribute in a promiscuous way not only in pure [3, 2], but also in *mixed* symmetric three-mode Gaussian states. However, the global mixedness is prone to affect this sharing structure, which is completely destroyed if, as can be seen from Eq. (14), the global purity μ falls below $1/(3\sqrt{3}) \approx 0.19245$. This purity threshold is remarkably low: a really strong amount of global noise is necessary to destroy the promiscuity of entanglement distribution.

We will now provide an example of three-mode states with weaker symmetry constraints, where the entanglement exhibits a more traditional sharing structure, *i.e.* with bipartite and tripartite quantum correlations being mutual competitors.

3.2. Promiscuity versus lack of symmetry: basset hound states

Let us consider here an instance of tripartite entangled states which are not fully symmetric, but merely bisymmetric pure Gaussian states. Bisymmetry (a property definable for $M \times N$ Gaussian states [9]) means in this case invariance under the exchange of modes 2 and 3, and not under the exchange of *any* two modes as in the previous (pure and mixed) GHZ/W instances.

Following the arguments summarized in Fig. 2, bisymmetric Gaussian states will be in general referred to as *basset hound* states. To our aims, it is sufficient here to consider *pure* basset hound states$^+$. Such states are characterised by a CM $\boldsymbol{\sigma}_B^p$ of the form Eq. (1), with

$$\boldsymbol{\sigma}_1 = a\mathbb{1}_2, \qquad \boldsymbol{\sigma}_2 = \boldsymbol{\sigma}_3 = \left(\frac{a+1}{2}\right)\mathbb{1}_2, \tag{16}$$

$$\boldsymbol{\varepsilon}_{23} = \left(\frac{a-1}{2}\right)\mathbb{1}_2, \quad \boldsymbol{\varepsilon}_{12} = \boldsymbol{\varepsilon}_{13} = \mathrm{diag}\left\{\frac{\sqrt{a^2-1}}{\sqrt{2}}, -\frac{\sqrt{a^2-1}}{\sqrt{2}}\right\}. \tag{17}$$

They belong to a family of states introduced in Ref. [31] as resources for optimal CV telecloning (*i.e.* cloning at distance, or equivalently teleportation to more than one receiver) of single-mode coherent states. We shall discuss this protocol in detail in Sec. 7.

¶ The noise expressed in decibels (dB) is obtained from the covariance matrix elements via the formula $N_{ij}(dB) = 10\log_{10}(\sigma_{ij})$.

$^+$ Unless explicitly stated, we will always assume in the following that the expression "basset hound state" denotes a *pure* bisymmetric Gaussian state. Notice that the possibility of unitary localization is common to all pure states [28, 29, 30] and is not specifically related – *for pure states* – to their symmetry properties.

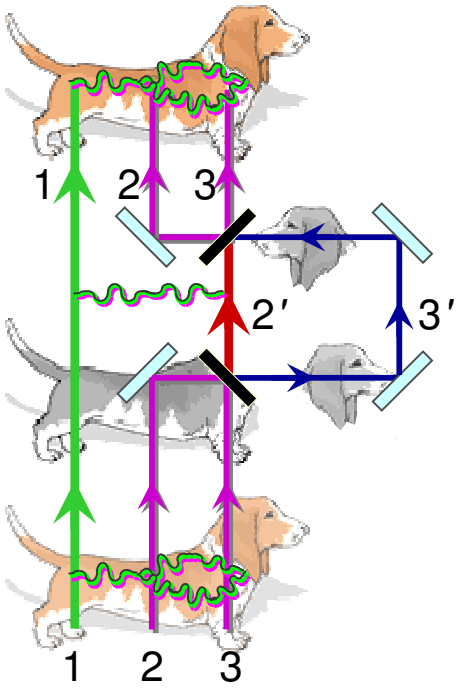

Figure 2. IF YOU CUT THE HEAD OF A BASSET HOUND, IT WILL GROW AGAIN [27]. Graphical depiction of the process of unitary localization (concentration) and delocalization (distribution) of entanglement in three-mode bisymmetric Gaussian states [9] (or "basset hound" states), described in the text. Initially, mode 1 is entangled (entanglement is depicted as a waving string) with both modes 2 and 3. It exists a local (with respect to the $1|(23)$ bipartition) symplectic operation, realized *e.g.* via a beam-splitter (denoted by a black thick dash), such that all the entanglement is concentrated between mode 1 and the transformed mode $2'$, while the other transformed mode $3'$ decouples from the rest of the system (*unitary localization*). Therefore, the head of the basset hound (mode $3'$) has been cut off. However, being realized through a symplectic operation (*i.e.* unitary on the density matrix), the process is reversible: operating on modes $2'$ and $3'$ with the inverse symplectic transformation, yields the original modes 2 and 3 entangled again with mode 1, without any loss of quantum correlations (*unitary delocalization*): the head of the basset hound is back again.

3.2.1. Tripartite entanglement From a qualitative point of view, basset hound states are fully inseparable for $a > 1$ and fully separable for $a = 1$, as already remarked in Ref. [31]; moreover, the PPT criterion entails that the two-mode reduced state of modes 2 and 3 is always separable. Following the guidelines of Sec. 2.1, the residual Gaussian contangle G_τ^{res} of such states is easily computable. As we know [3], the minimum in Eq. (5) is attained by choosing as probe the mode of smallest local mixedness. In our setting, this corresponds to set either mode 2 or mode 3 (indifferently, due to the bisymmetry) to be the probe mode. Let us choose mode 3; then we have

$$G_\tau^{res}(\boldsymbol{\sigma}_B^p) = G_\tau^{3|(12)}(\boldsymbol{\sigma}_B^p) - G_\tau^{3|1}(\boldsymbol{\sigma}_B^p)\,, \tag{18}$$

with

$$G_\tau^{3|(12)}(\boldsymbol{\sigma}_B^p) = \mathrm{arcsinh}^2\left[\frac{1}{2}\sqrt{(a-1)(a+3)}\right]\,, \tag{19}$$

$$G_\tau^{3|1}(\boldsymbol{\sigma}_B^p) \quad = \operatorname{arcsinh}^2\left[\sqrt{\frac{(3a+1)^2}{(a+3)^2}-1}\right]. \tag{20}$$

The tripartite entanglement of Eq. (18) is strictly smaller than that of GHZ/W states, but it can still diverge in the limit of infinite squeezing ($a \to \infty$) due to the global purity of these basset hound states. Instead, the bipartite entanglement $G_\tau^{1|2} = G_\tau^{1|3}$ between mode 1 and each of the modes 2 and 3 in the corresponding two-mode reductions, given by Eq. (20), is strictly *larger* than the bipartite entanglement in any two-mode reduction of GHZ/W states. This does not contradict the previously given characterization of GHZ/W states as maximally three-way and two-way entangled (maximally promiscuous). In fact, GHZ/W states have maximal couplewise entanglement between *any* two-mode reduction, while in basset hound states only two (out of three) two-mode reductions are entangled, allowing this entanglement to be larger. This is the reason why these states are well-suited for telecloning, as we will detail in Sec. 7.1. Nevertheless, this reduced bipartite entanglement cannot increase arbitrarily in the limit of infinite squeezing, because of the monogamy inequality satisfied by the Gaussian contangle. In fact, it saturates to

$$G_\tau^{1|l}(\boldsymbol{\sigma}_B^p,\, a \to \infty) = \ln^2\left[3+2\sqrt{2}\right] \approx 3.1\,, \tag{21}$$

which is about ten times the asymptotic value of the reduced bipartite two-mode entanglement for GHZ/W states, Eq. (8).

3.2.2. Sharing structure It is interesting to notice that entanglement sharing in basset hound states is *not* promiscuous. Tripartite and bipartite entanglement coexist (the latter only in two of the three possible two-mode reductions), but the presence of a strong bipartite entanglement does not help the tripartite one to be stronger (at fixed local mixedness a) than in other states, like GHZ/W states or even T states [3] (which are globally mixed and moreover contain no reduced bipartite entanglement at all).

3.3. The origin of tripartite entanglement promiscuity?

The above analysis of the entanglement sharing structure in three-mode Gaussian states (including the non-fully-symmetric basset hound states, whose entanglement structure is not promiscuous) delivers a clear hint that, in the tripartite Gaussian setting, *'promiscuity'* is a peculiar consequence not of the global purity (noisy GHZ/W states remain promiscuous for quite strong mixedness), but of the complete *symmetry* under modes-exchange. Beside frustrating the maximal entanglement between pairs of modes [32], symmetry also constrains the multipartite sharing of quantum correlations. In basset hound states (bisymmetric Gaussian states), the separability of the reduced state of modes 2 and 3 prevents the three modes from having a strong genuine tripartite entanglement among them all, despite the heavy quantum correlations shared by the two couples of modes $1|2$ and $1|3$.

It is instructive to recall that, obviously, fully symmetric states are bisymmetric under any bipartition of the modes: pictorially (see Fig. 2), they are thus a special type of basset hound state resembling a *Cerberus* state, in which any one of the three heads can be cut and can be reversibly regrown. Only in this case can a promiscuous sharing of entanglement arise. It is worth stressing that fully symmetric Gaussian states include nearly all the states of tripartite CV systems currently produced in the laboratory by quantum optical means [33, 34]; we will discuss their usefulness as resources for quantum communication protocols with continuous variables in Sec. 6.

Let us also mention that the argument connecting promiscuous entanglement to complete permutation invariance does not hold anymore in the case of Gaussian states with four and more modes, where relaxing the symmetry constraints allows for an *enhancement* of the distributed entanglement promiscuity to an unlimited extent [23] (thanks to the greater freedom available in a 8-dimensional phase space).

4. Optical production of three-mode Gaussian states

In this Section, we present a novel (and more economical, in a well-defined sense, with respect to previous proposals) recipe to generate pure three-mode Gaussian states with any, arbitrary, entanglement structure. Moreover, we provide a systematic analysis of state engineering of the classes of three-mode Gaussian states – characterized by peculiar structural and/or entanglement properties – introduced in the previous section and in Ref. [2]. For every family of Gaussian states, we shall outline schemes for their production with current optical technology [35].

4.1. The "allotment" box for the production of arbitrary three-mode pure states

The investigation of the structural properties and the computation of the tripartite entanglement, quantified by the residual Gaussian contangle of Eq. (5) (arravogliament), in general *pure* three-mode Gaussian states has been presented in full detail in Ref. [2]. Here we investigate how to engineer these states with optical means, allowing for any possible entanglement structure.

A viable scheme to produce all pure three-mode Gaussian states, as inspired by Euler decomposition [36], would combine three independent squeezed modes (with in principle all different squeezing factors) into any conceivable combination of orthogonal (energy preserving) symplectic operations (essentially, beam-splitters and phase-shifters). This procedure, that is obviously legitimate and will surely be able to generate any pure state, is however not, in general, the most economical one in terms of physical resources. Moreover, this procedure is not particularly insightful because the degrees of bipartite and tripartite entanglement of the resulting output states is not, in general, easily related to the performed operations.

In this section, we want instead to give a precise recipe providing the exact operations to achieve a three-mode pure Gaussian state with any given triplet $\{a_1,\, a_2,\, a_3\}$ of local mixedness, and so with any desired 'physical' (*i.e.* , constrained by Inequality (6)) asymmetry among the three modes and any needed amount of tripartite entanglement. Clearly, such a recipe is *not* unique.* We provide here one possible, novel scheme, which may not be the cheapest one but possesses a straightforward physical interpretation: the passive distribution, or *allotment* of two-mode entanglement among three modes.

Explicitly, one starts with modes 1 and 2 in a two-mode squeezed state (which can be obtained in the lab [38], either directly in non-degenerate parametric processes or by mixing two squeezed vacua at a beam-splitter), and mode 3 in the vacuum state. In Heisenberg picture:

$$\hat{q}_1 = \frac{1}{\sqrt{2}} \left(e^r \, \hat{q}_1^0 + e^{-r} \, \hat{q}_2^0 \right) , \quad \hat{p}_1 = \frac{1}{\sqrt{2}} \left(e^{-r} \, \hat{p}_1^0 + e^r \, \hat{p}_2^0 \right) , \tag{22}$$

* An alternative scheme to produce pure three-mode Gaussian states can be inferred from Ref. [37], where the state engineering of pure N-mode Gaussian states with no correlations between position and momentum operators is discussed. We will discuss it in comparison with the present scheme, later in the text.

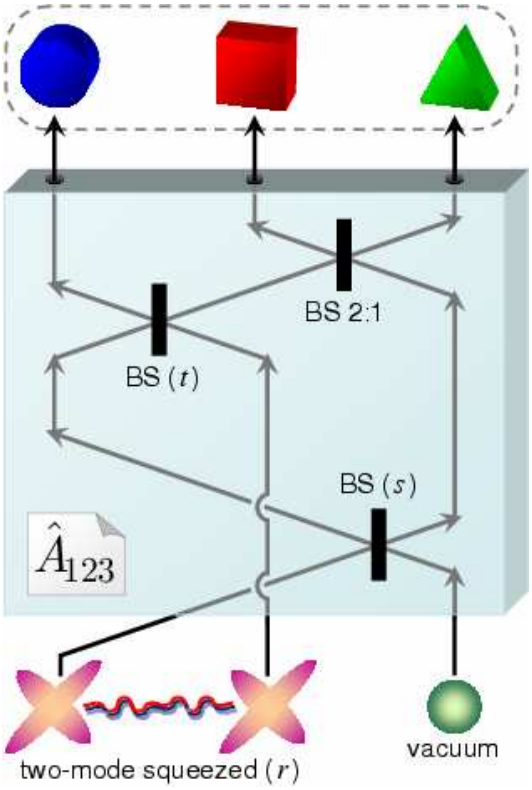

Figure 3. Scheme to produce arbitrary pure three-mode Gaussian states (up to local unitaries). A two-mode squeezed state and a single-mode vacuum are combined by the "allotment" operator $\hat{A}_{123}$, which is a sequence of three beam-splitters, Eq. (25). The output yields an arbitrary pure Gaussian state of modes 1 (blue circle ●), 2 (red square ■), and 3 (green triangle ▲), whose CM depends on the initial squeezing factor $m = \cosh(2r)$ and on two beam-splitter transmittivities s and t.

$$\hat{q}_2 = \frac{1}{\sqrt{2}}\left(e^r\ \hat{q}_1^0 - e^{-r}\ \hat{q}_2^0\right)\ , \quad \hat{p}_2 = \frac{1}{\sqrt{2}}\left(e^{-r}\ \hat{p}_1^0 - e^r\ \hat{p}_2^0\right)\ , \tag{23}$$

$$\hat{q}_3 = \hat{q}_3^0\ , \qquad \hat{p}_3 = \hat{p}_3^0\ , \tag{24}$$

where the suffix "0" refers to the vacuum.

The three initial modes are then sent in a sequence of three beam-splitters, which altogether realize what we will call "allotment" operator and denote by $\hat{A}_{123}$ (see Fig. 3):

$$\hat{A}_{123} \equiv \hat{B}_{23}(\arccos\sqrt{2/3}) \cdot \hat{B}_{12}(\arccos\sqrt{t}) \cdot \hat{B}_{13}(\arccos\sqrt{s})\ . \tag{25}$$

Here the action of an ideal (phase-free) beam-splitter operation $\hat{B}_{ij}$ on a pair of modes i and j is defined as

$$\hat{B}_{ij}(\theta) : \begin{cases} \hat{a}_i \to \hat{a}_i \cos\theta + \hat{a}_j \sin\theta \\ \hat{a}_j \to \hat{a}_i \sin\theta - \hat{a}_j \cos\theta \end{cases}\ , \tag{26}$$

with $\hat{a}_l = (\hat{x}_l + i\hat{p}_l)/2$ being the annihilation operator of mode k, and θ the angle in phase space ($\theta = \pi/4$ corresponds to a 50:50 beam-splitter).

It is convenient in this instance to deal with the phase-space representations of the states (*i.e.* their CM) and of the operators (*i.e.* the associated symplectic transformations). The three-mode input state is described by a CM $\boldsymbol{\sigma}_{in}^{p}$ of the form Eq. (1) for $n = 3$, with

$$\boldsymbol{\sigma}_1 = \boldsymbol{\sigma}_2 = m\ \mathbb{1}_2\,, \qquad \boldsymbol{\sigma}_3 = \mathbb{1}_2\,, \tag{27}$$

$$\boldsymbol{\varepsilon}_{12} = \mathrm{diag}\left\{\sqrt{m^2-1},\,-\sqrt{m^2-1}\right\}\,, \quad \boldsymbol{\varepsilon}_{13} = \boldsymbol{\varepsilon}_{23} = \mathbf{0}\,, \tag{28}$$

and $m \equiv \cosh(2r)$. A beam-splitter with transmittivity τ corresponds to a rotation of $\theta = \arccos\sqrt{\tau}$ in phase space, see Eq. (26). In a three-mode system, the symplectic transformation corresponding to $\hat{B}_{ij}(\theta)$ is a direct sum of the matrix $B_{ij}(\tau)$,

$$B_{ij}(\tau) = \begin{pmatrix} \sqrt{\tau} & 0 & \sqrt{1-\tau} & 0 \\ 0 & \sqrt{\tau} & 0 & \sqrt{1-\tau} \\ \sqrt{1-\tau} & 0 & -\sqrt{\tau} & 0 \\ 0 & \sqrt{1-\tau} & 0 & -\sqrt{\tau} \end{pmatrix}\,, \tag{29}$$

acting on modes i and j, and of the identity $\mathbb{1}_2$ acting on the remaining mode k.

The output state after the allotment will be denoted by a CM $\boldsymbol{\sigma}_{out}^{p}$ given by

$$\boldsymbol{\sigma}_{out}^{p} = A_{123}\boldsymbol{\sigma}_{in}^{p}A_{123}^{\mathsf{T}}\,, \tag{30}$$

where A_{123} is the phase-space representation of the allotment operator Eq. (25), obtained from the matrix product of the three beam-splitter transformations. The output state is clearly pure because the allotment is a unitary operator (symplectic in phase space). The elements of the CM $\boldsymbol{\sigma}_{out}^{p}$, not reported here for brevity, are functions of the three parameters

$$m \in [1,\,\infty), \quad s \in [0,\,1], \quad t \in [0,\,1]\,. \tag{31}$$

In fact, by letting these three parameters vary in their respective domain, the presented procedure allows for the creation of three-mode pure Gaussian states with any possible triplet of local mixednesses $\{a_1,\,a_2,\,a_3\}$ ranging in the physical region defined by the triangle inequality (6), and thus encompassing all the possible entanglement structures, under any partition of the system.

This can be shown as follows. Once identified $\boldsymbol{\sigma}_{out}^{p}$ with the block form of Eq. (1) (for $n = 3$), one can solve analytically the equation $\mathrm{Det}\,\boldsymbol{\sigma}_1 = a_1^2$ to find

$$m(a_1, s, t) = \frac{t\big(t(s-1)^2+s-1\big)+\sqrt{a_1^2(st+t-1)^2+4s(t-1)t(2t-1)(2st-1)}}{(st+t-1)^2}\,. \tag{32}$$

Then, substituting Eq. (32) in $\boldsymbol{\sigma}_{out}^{p}$ yields a reparametrization of the output state in terms of a_1 (which is given), s and t. Now solve (numerically) the system of nonlinear equations $\{\mathrm{Det}\,\boldsymbol{\sigma}_2 = a_2^2,\,\mathrm{Det}\,\boldsymbol{\sigma}_3 = a_3^2\}$ in the variables s and t. Finally, substitute back the obtained values of the two transmittivities in Eq. (32), to have the desired triplet $\{m,\,s,\,t\}$ as functions of the local mixednesses $\{a_1,\,a_2,\,a_3\}$ characterizing the target state.

An arbitrary pure three-mode Gaussian state, with a CM locally equivalent to the standard form of Eq. (1) with all diagonal 2×2 subblocks, can thus be produced with the current experimental technology by linear quantum optics, employing the allotment box with exactly tuned amounts of input two-mode squeezing and beam-splitter properties, without any free parameter left. The outcome of this procedure is shown in Fig. 4, where at a given local mixedness of mode 1 ($a_1 = 2$), several runs of the allotment operator have been simulated adopting beam-splitters of random transmittivities s and t. Starting from a two-mode squeezed input with m given by Eq. (32), tensor a vacuum, the resulting output states are plotted in the space of a_2 and a_3. By comparing Fig. 4 with Fig. 1 of Ref. [2], one sees clearly that the randomly generated states distribute towards a complete fill of the physical region emerging from the triangle inequality (6), thus confirming the generality of our scheme.

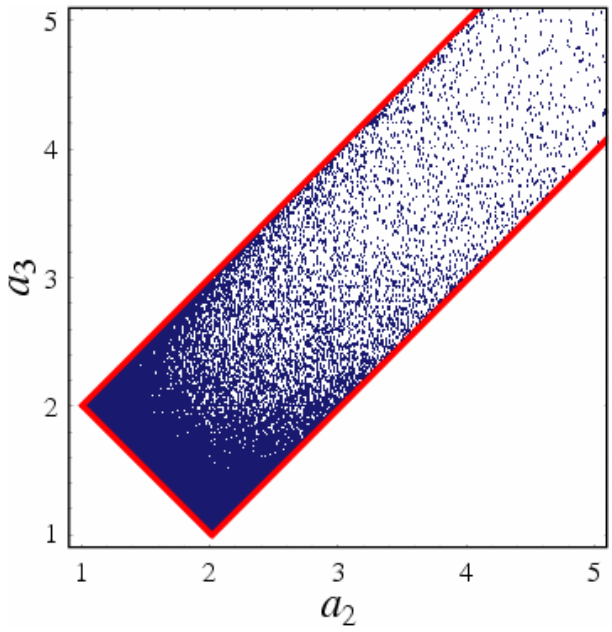

Figure 4. Plot of 100000 randomly generated pure three-mode Gaussian states, described by their single-mode mixednesses a_2 and a_3, at fixed $a_1 = 2$. The states are produced by simulated applications of the allotment operator with random beam-splitter transmittivities s and t, and span the whole physical range of parameters allowed by Ineq. (6). A comparison of this plot with Fig. 1 of Ref. [2] may be instructive. See text for further details.

A remark is in order here. The optical scheme presented in Ref. [37] to produce pure N-mode Gaussian states with "generic entanglement" (corresponding to standard form CMs with null position-momentum covariances), also allows in the special case of $N = 3$ for the creation of *all* pure three-mode Gaussian states with CM in standard form (see Sec. 2 and Ref. [2]). Therefore, such a state engineering recipe represents an alternative to the allotment box of Fig. 3. However, there is a crucial difference between the two schemes: the allotment box requires *in toto* (considering both the preparation and the further manipulation of the input states out of three vacuum beams) a single "active" (*i.e.* non energy-preserving), squeezing operation, whereas the scheme of Ref. [37] needs two squeezing operations to be accomplished. In this specific sense, the allotment strategy is "more economical" over the scheme of Ref. [37] (in view of the superior expediency with which passive operations – beam-splitters, in this instance – can be realized in practice, being considerably more efficient and reliable than squeezings). More in detail, in both schemes, the input in modes 1 and 2 is a two-mode squeezed state, whose squeezing parameter accounts for one of the three degrees of freedom of pure three-mode Gaussian states in standard form. Still, while in the present scheme mode 3 starts off in the vacuum state, the scheme of Ref. [37] requires an initial single-mode squeezed state in mode 3: a single beam-splitter (between modes 2 and 3) is then enough to achieve a completely general entanglement structure. On the other hand, the allotment box presented here is realized by a *passive* redistribution of entanglement only, as the third mode is not squeezed, but the three modes need to interfere with each other via three beam-splitters (one of which has fixed transmittivity) and this again yields a completely general entanglement freedom. Summing up, the allotment scheme presented here needs four operations, three of

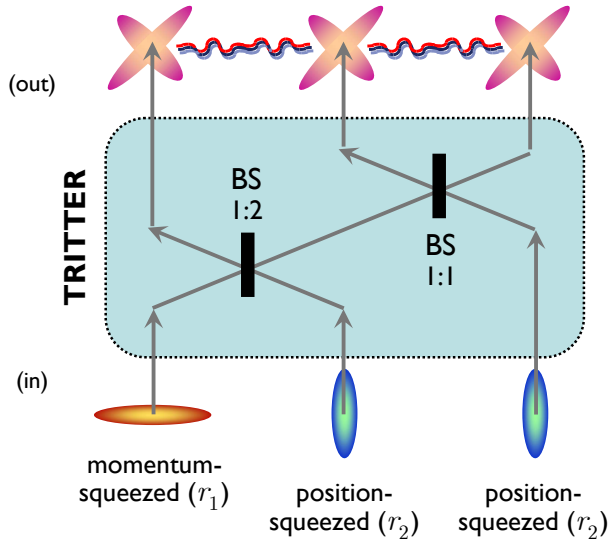

Figure 5. Scheme to produce CV GHZ/W states, as proposed in Ref. [39] and implemented in Ref. [33]. Three independently squeezed beams, one in momentum and two in position, are combined through a double beam-splitter (tritter). The output yields a pure, symmetric, fully inseparable three-mode Gaussian state, also known as CV GHZ/W state.

which are passive, while the scheme of Ref. [37] needs two active operations and one passive operation to achieve full generality. Depending on the specific experimental facilities, one may thus choose either scheme when aiming to produce pure three-mode Gaussian states. Clearly, if a very high amount of final entanglement is required, the strategy adopting *two* squeezing operations in lieu of one might be more suitable (as the squeezing achievable in a single parametric process is limited); however, such larger entanglement will come at the price of a considerably higher level of noise (as parametric processes are generally less stable than passive linear optics).

4.2. Concise guide to tripartite state engineering and simplified schemes

Let us now turn to the production of the classes of three-mode states introduced in Sec. 3 and in Ref. [2]. For mixed instances of such tripartite states (not subsumed by the allotment operator), efficient state engineering schemes will be outlined. Also, in special instances of pure states, depending in general on less than three parameters, cheaper recipes than the general one in terms of the allotment box will be presented.

4.2.1. Pure and noisy GHZ/W states Several schemes have been proposed to produce pure GHZ/W states with finite squeezing [3, 2], *i.e.* fully symmetric pure three-mode Gaussian states (with promiscuous entanglement sharing). In particular, as discussed by Van Loock and Braunstein [39], these states can be produced by mixing three squeezed beams (one in momentum and the other two in position) in a double beam-splitter, or *tritter* [40].

One starts with mode 1 squeezed in momentum, and modes 2 and 3 squeezed in position. In Heisenberg picture:

$$\hat{q}_1 = e^{r_1}\,\hat{q}_1^0\,, \qquad \hat{p}_1 = e^{-r_1}\,\hat{p}_1^0\,, \tag{33}$$

$$\hat{q}_{2,3} = e^{-r_2}\,\hat{q}_{2,3}^0\,, \quad \hat{p}_{2,3} = e^{r_2}\,\hat{p}_{2,3}^0\,, \tag{34}$$

where the suffix "0" refers to the vacuum. Then one combines the three modes in a tritter

$$\hat{B}_{123} \equiv \hat{B}_{23}(\pi/4) \cdot \hat{B}_{12}(\arccos\sqrt{1/3})\,, \tag{35}$$

where the action of an ideal (phase-free) beam-splitter operation $\hat{B}_{ij}$ on a pair of modes i and j is defined by Eq. (26).

The output of the tritter yields a CM of the form Eq. (2) with

$$\boldsymbol{\alpha} = \mathrm{diag}\left\{\frac{1}{3}\left(e^{2r_1}+2e^{-2r_2}\right)\,,\quad \frac{1}{3}\left(e^{-2r_1}+2e^{2r_2}\right)\right\}\,, \tag{36}$$

$$\boldsymbol{\varepsilon} = \mathrm{diag}\left\{\frac{1}{3}\left(e^{2r_1}-e^{-2r_2}\right)\,,\quad \frac{1}{3}\left(e^{-2r_1}-e^{2r_2}\right)\right\}\,. \tag{37}$$

This resulting pure and fully symmetric three-mode Gaussian state, obtained in general with differently squeezed inputs $r_1 \neq r_2$, is locally equivalent to the state prepared with all initial squeezings equal to the average $\bar{r} = (r_1 + r_2)/2$ [41]. The CM described by Eqs. (36,37) represents a CV GHZ/W state. It can be in fact transformed, by local symplectic operations, into the standard form CM of Ref. [2], which obeys Eq. (2) with $a \equiv \sqrt{\mathrm{Det}\,\boldsymbol{\alpha}}$ given by

$$a = \frac{1}{3}\sqrt{4\cosh\left[2\left(r_1+r_2\right)\right]+5}\,. \tag{38}$$

Noisy GHZ/W states, whose entanglement has been characterized in Sec. 3.1, can be obviously obtained by an analogous procedure starting from (Gaussian) thermal states instead of vacua (with average photon number $\bar{n} = [n-1]/2 \geq 0$) and combining them through a tritter Eq. (35). The initial single, separable, modes are thus described by the following operators in Heisenberg picture (we will now assume the same squeezing parameter $\bar{r} \equiv r$ for the three beams, as it allows for any case of noisy GHZ/W states up to local unitaries)

$$\hat{q}_1 = \sqrt{n}e^{r}\,\hat{q}_1^0\,, \qquad \hat{p}_1 = \sqrt{n}e^{-r}\,\hat{p}_1^0\,, \tag{39}$$

$$\hat{q}_{2,3} = \sqrt{n}e^{-r}\,\hat{q}_{2,3}^0\,, \quad \hat{p}_{2,3} = \sqrt{n}e^{r}\,\hat{p}_{2,3}^0\,. \tag{40}$$

Defining $s \equiv e^{2r}$, at the output of the tritter one obtains a CM of the form Eq. (2), with

$$\boldsymbol{\alpha} = \mathrm{diag}\left\{\frac{n(s^2+2)}{3s}\,,\quad \frac{n(2s^2+1)}{3s}\right\}\,, \tag{41}$$

$$\boldsymbol{\varepsilon} = \mathrm{diag}\left\{\frac{n(s^2-1)}{3s}\,,\quad -\frac{n(s^2-1)}{3s}\right\}\,. \tag{42}$$

This resulting CM is locally equivalent to the standard form of of Ref. [2], which obeys Eq. (2) with $a \equiv \sqrt{\mathrm{Det}\,\boldsymbol{\alpha}}$ given by

$$a = \frac{n\sqrt{2s^4+5s^2+2}}{3s}\,. \tag{43}$$

Clearly, setting $n = 1$ corresponds to the case of pure GHZ/W states.

The preparation scheme of CV GHZ/W states is depicted in Fig. 5. It has has been experimentally implemented [33], and the full inseparability of the produced states has been verified through the violation of the separability inequalities derived in Ref. [15]. Very recently, the production of strongly entangled GHZ/W states has also been demonstrated by using a novel optical parametric oscillator, based on concurrent $\chi^{(2)}$ nonlinearities [34].

4.2.2. T states The T states have been introduced in Refs. [2, 3] to show that, in symmetric three-mode Gaussian states, imposing the absence of reduced bipartite entanglement between any two modes results in a frustration of the genuine tripartite entanglement. It may be useful to know how to produce this novel class of mixed, fully symmetric Gaussian states in the lab.

The simplest way to engineer T states is to reutilize the scheme of Fig. 5, *i.e.* basically the tritter of Eq. (35), but with different inputs. Namely, one has mode 1 squeezed again in momentum (with squeezing parameter r), but this time modes 2 and 3 are in a thermal state (with average photon number $\bar{n} = [n(r) - 1]/2$, depending on r). In Heisenberg picture:

$$\hat{q}_1 = e^r \, \hat{q}_1^0 \, , \qquad \hat{p}_1 = e^{-r} \, \hat{p}_1^0 \, , \tag{44}$$

$$\hat{q}_{2,3} = \sqrt{n(r)} \, \hat{q}_{2,3}^0 \, , \quad \hat{p}_{2,3} = \sqrt{n(r)} \, \hat{p}_{2,3}^0 \, , \tag{45}$$

with $n(r) = \sqrt{3 + e^{-4r}} - e^{-2r}$. Sending these three modes in a tritter Eq. (35) one recovers, at the output, a T state whose CM is locally equivalent to the standard form of Ref. [2], with

$$a = \frac{1}{3} \sqrt{2e^{-2r} \sqrt{3 + e^{-4r}} \, (-3 + e^{4r}) + 6e^{-4r} + 11} \, . \tag{46}$$

4.2.3. Basset hound states A scheme for producing the basset hound states of Sec. 3.2, and in general the whole family of pure bisymmetric Gaussian states known as "multiuser quantum channels" (due to their usefulness for telecloning, as we will show in Sec. 7), is provided in Ref. [31]. In the case of three-mode pure basset hound states of the form given by Eqs. (16,17), one can use a simplified version of the allotment introduced in Sec. 4.1 for arbitrary pure states. One starts with a two-mode squeezed state (with squeezing parameter r) of modes 1 and 2, and mode 3 in the single-mode vacuum, like in Eqs. (22–24). Then, one combines one half (mode 2) of the two-mode squeezed state with the vacuum mode 3 via a 50:50 beam-splitter, described in phase space by $B_{23}(1/2)$ of Eq. (29). The resulting three-mode state is exactly a basset hound state described by Eqs. (16,17), once one identifies $a \equiv \cosh(2r)$. In a realistic setting, dealing with noisy input modes, mixed bisymmetric states can be obtained as well by the same procedure.

5. Application: Multiparty quantum teleportation with continuous variables

We now address more closely the usefulness of three-mode Gaussian states for the efficient implementation of quantum information and communication protocols. In particular, we intend to provide the theoretical entanglement characterization of three-mode Gaussian states with a significant operative background and to epitomize their capability for quantum communication tasks. To this aim, we shall focus on the transmission of quantum states within a network of three parties which share entangled Gaussian resources.

For two parties, the process of *quantum teleportation* using entanglement and with the aid of classical communication was originally proposed for qubit systems [42], and experimentally implemented with polarization-entangled photons [43, 44]. The CV counterpart of discrete-variable teleportation, using quadrature entanglement, is in principle imperfect due to the impossibility of achieving infinite squeezing. Nevertheless, by considering the finite EPR correlations between the quadratures of a two-mode squeezed Gaussian state, a realistic scheme for CV teleportation (see Ref. [45] for a recent review) was proposed [46, 47] and experimentally implemented [48] to teleport coherent states with a measured fidelity $\mathcal{F} = 0.70 \pm 0.02$ [49]. Without using entanglement, by purely classical communication, an average fidelity of

$$\mathcal{F}_{cl} = \frac{1}{2} \tag{47}$$

is the maximal achievable with an alphabet of uniformly distributed coherent input states [50, 51]. Let us recall that the fidelity $\mathcal{F}$, which is the figure of merit quantifying the success of a teleportation experiment, is defined with respect to a pure state $|\psi^{in}\rangle$ as

$$\mathcal{F} \equiv \langle\psi^{in}|\varrho^{out}|\psi^{in}\rangle\,. \tag{48}$$

Here "in" and "out" denote the input and the output states (the latter being generally mixed) of a teleportation process, respectively. $\mathcal{F}$ reaches unity only for a perfect state transfer, $\varrho^{out} = |\psi^{in}\rangle\langle\psi^{in}|$. To accomplish teleportation with high fidelity, the sender (Alice) and the receiver (Bob) must share an entangled state (resource). The *sufficient* fidelity criterion [50] states that, if teleportation is performed with $\mathcal{F} > \mathcal{F}_{cl}$, then the two parties exploited an entangled state. The converse is generally false: that is, quite surprisingly, some entangled resources may yield lower-than-classical fidelities [41, 39]. This point will be discussed thoroughly in the following.

To generalize the process of CV teleportation from two to three (and more) users, one can consider two basic possible scenarios. On the one hand, a network may be created where each user is able to teleport states with better-than-classical efficiency (being the same for all sender/receiver pairs) to any chosen receiver *with the assistance of the other parties*. On the other hand, one of the parties may act as the fixed sender, and distribute approximate copies (with in principle different cloning fidelities) to all the others acting as remote receivers. These two protocols, respectively referred to as "teleportation network" [39] and "telecloning" [31], will be described in the two following sections, and the connections between their successful implementation with three-mode Gaussian resources and the amounts of shared bipartite and tripartite entanglement will be elucidated. We just mention that several interesting variants to these basic schemes do exist (see, *e.g.* the 'cooperative telecloning' of Ref. [52], where two receivers – instead of two senders – are cooperating).

6. Teleportation networks with fully symmetric resources

The original CV teleportation protocol [47] has been generalized to a multi-user teleportation network requiring multiparty entangled Gaussian states in Ref. [39]. This network has been recently experimentally demonstrated by exploiting three-mode squeezed states (namely, noisy CV GHZ/W states, extensively addressed in section 3.1, were employed), yielding a maximal fidelity $\mathcal{F} = 0.64 \pm 0.02$ [53].

In Ref. [41] the problem was raised of determining the *optimal* multi-user teleportation fidelity (in the general N-mode setting), and to extract from it a quantitative information on the multipartite entanglement in the shared resource. The optimization consists in a maximization of the fidelity over all local single-mode operations ('pre-processing' the initial resource), at fixed amounts of noise and entanglement in the shared resource. This is motivated by the simple observation that states equivalent up to local single-mode unitary operations (which possess, by definition, the same amount of bipartite and multipartite entanglement with respect to any partition) behave in general differently when employed in a fixed (not locally optimized) quantum information protocol.♯ In the previous section, dedicated to state engineering, we provided schemes for the generation of states with CMs *locally equivalent* to the corresponding standard forms. The teleportation efficiency, instead, depends separately on the different single-mode properties (in particular, on the squeezings degrees of the input states before combining them via optical networks like the tritter or the allotment).

♯ Clearly, this fact is, *per se*, not that surprising. Also, it may be noted that one could, having a complete knowledge about the resource, always include the local optimizing pre-processing as the first step of the considered "protocol".

For fully symmetric (pure or mixed) shared resource, it has been shown in Ref. [41] that the optimal fidelity $\mathcal{F}_N^{opt}$ obtained in such way is *equivalent* to the presence of genuine multipartite entanglement in the shared resource. This results yield quite naturally a direct operative way to quantify multipartite entanglement in N-mode (mixed) symmetric Gaussian states, in terms of the so-called *Entanglement of Teleportation*, defined as the normalized optimal fidelity

$$E_T^{(N)} \equiv \max\left\{0, \frac{\mathcal{F}_N^{opt} - \mathcal{F}_{cl}}{1 - \mathcal{F}_{cl}}\right\}, \tag{49}$$

with $\mathcal{F}_{cl} \equiv 1/2$ being the classical threshold For any N, the entanglement of teleportation ranges from 0 (separable resource states) to 1 (CV generalized GHZ resource state, simultaneous eigenstate of total momentum and all relative positions of the N-mode radiation field). As we will discuss in detail later on, the equivalence between optimal fidelity of teleportation and entanglement breaks down in the asymmetric instance, even for two-mode states.

We shall now remind a particular relationship (first found in Ref. [41]) between the entanglement of teleportation and the residual Gaussian contangle introduced in Sec. 2.1 and further discuss its operational consequences in terms of teleportation networks, eventually leading to a proposal to experimentally test the promiscuous sharing of correlations with three-mode Gaussian states.

6.1. On the operational interpretation of tripartite Gaussian entanglement and on how to experimentally investigate its sharing structure

6.1.1. Entanglement of teleportation and residual contangle Let us focus, for the following discussion, on the case $N = 3$, *i.e.* on three-mode states shared as resources for a three-party teleportation network. This protocol is a basic, natural candidate to operationally investigate the sharing structure of CV entanglement in three-mode symmetric Gaussian states.

A first theoretical question that arises is to compare the tripartite entanglement of teleportation Eq. (49), which is endowed with a strong operational motivation [41], and the tripartite residual (Gaussian) contangle Eq. (5), which is built on solid mathematical foundations. Remarkably, in the case of *pure* and *symmetric* three-mode resources (*i.e.* for CV GHZ/W states) the two measures are completely equivalent [41], being monotonically increasing functions of each other. Namely, from Eq. (7),

$$G_\tau^{res}(\boldsymbol{\sigma}_s^{\mathrm{GHZ}/W}) = \ln^2 \frac{2\sqrt{2}E_T - (E_T+1)\sqrt{E_T^2+1}}{(E_T-1)\sqrt{E_T(E_T+4)+1}} - \frac{1}{2}\ln^2 \frac{E_T^2+1}{E_T(E_T+4)+1}, \tag{50}$$

where $E_T \equiv E_T^{(3)}$ in Eq. (49). Let us moreover recall that G_τ^{res} coincides with the true residual contangle (globally minimized in principle over all, including non-Gaussian, decompositions), Eq. (4), in these states [3, 2].

Therefore, in the specific (but relevant) instance of symmetric pure states, the residual (Gaussian) contangle is enriched of an interesting meaning as a *resource* enabling a better-than-classical three-party teleportation experiment, while no operational interpretations are presently known for the three-way residual tangle quantifying tripartite entanglement sharing in qubit systems [19, 22]. We remark that in the tripartite instance, the optimal fidelity $\mathcal{F}_3^{opt}$ – determining the entanglement of teleportation – achieves indeed its *global* maximum over all possible Gaussian POVMs performed on the shared resource, as can be confirmed with the methods of Ref. [54].

6.1.2. The role of promiscuity in symmetric three-mode resources The relationship between optimal teleportation fidelity and residual (Gaussian) contangle, embodied by Eq. (50), entails that there is a 'unique' kind of three-party CV entanglement in pure *symmetric* three-mode Gaussian states (alias CV finite-squeezing GHZ/W states), which merges at least three (usually inequivalent) properties: those of being maximally genuinely tripartite entangled, maximally bipartite entangled in any two-mode reduction, and 'maximally efficient' (in the sense of the optimal fidelity) for three-mode teleportation networks. Recall that the first two properties, taken together, label such entanglement as *promiscuous*, as discussed in Sec. 6.1.2. These features add up to the property of tripartite GHZ/W Gaussian states of being maximally robust against decoherence effects among all three-mode Gaussian states, as shown in Ref. [2] and operatively demonstrated later in Sec. 6.2.

All this theoretical evidence strongly promotes GHZ/W states, experimentally realizable with current optical technology [33, 34] (see Sec. 4.2.1), as paradigmatic candidates for the encoding and transmission of CV quantum information and in general for reliable CV quantum communication. Let us mention that, in particular, these tripartite entangled symmetric Gaussian states have been successfully employed to demonstrate quantum secret sharing [55], controlled dense coding [56], and the above discussed teleportation network [53]. Quite recently, a theoretical solution for CV Byzantine agreement has been reported [57], based on the use of sufficiently entangled states from the family of CV GHZ/W states.

Building on our entanglement analysis, we can precisely enumerate the peculiarities of those states which make them so appealing for practical implementations. Exploiting a strongly entangled three-mode CV GHZ/W state as a quantum channel affords one with a number of simultaneous advantages:

(i) the "guaranteed success" (*i.e.* with better-than-classical figures of merit) of any known tripartite CV quantum information protocol;

(ii) the "guaranteed success" of any standard two-user CV protocol, because a highly entangled two-mode channel is readily available after a unitary (reversible) localization of entanglement has been performed through a single beam-splitter (see Fig. 2);

(iii) the "guaranteed success" (though with nonmaximal efficiency) of any two-party quantum protocol through each two-mode channel obtained discarding one of the three modes.

Point (iii) ensures that, even when one mode is lost, the remaining (mixed) two-mode resource can be still implemented for a two-party protocol with better-than-classical success. It is realized with nonmaximal efficiency because, as we have seen from Eq. (8), the reduced entanglement in any two-mode partition remains finite even with infinite squeezing (the reason why promiscuity of tripartite Gaussian entanglement is only "partial", compared to the four-partite case of Ref. [23]).

We can now readily provide an explicit proposal to implement the above checklist in terms of CV teleportation networks.

6.1.3. Testing the promiscuous sharing of tripartite entanglement The results just elucidated pave the way towards an experimental test for the promiscuous sharing of tripartite CV entanglement in symmetric Gaussian states, as anticipated in the outlook of Ref. [41].To unveil this peculiar feature, one should prepare a pure CV GHZ/W state according to Fig. 5, in the optimal form given by Ref. [41]. It is worth remarking that, in the case of three modes, non-optimal forms like that produced with $r_1 = r_2$ in Eqs. (33, 34) [33, 53] yield fidelities really close to the maximal one [see Fig. 6(a)], and are thus practically as good as the optimal states (if not even better, taking into account that the states with $r_1 = r_2$ are generally easier to produce in practice).

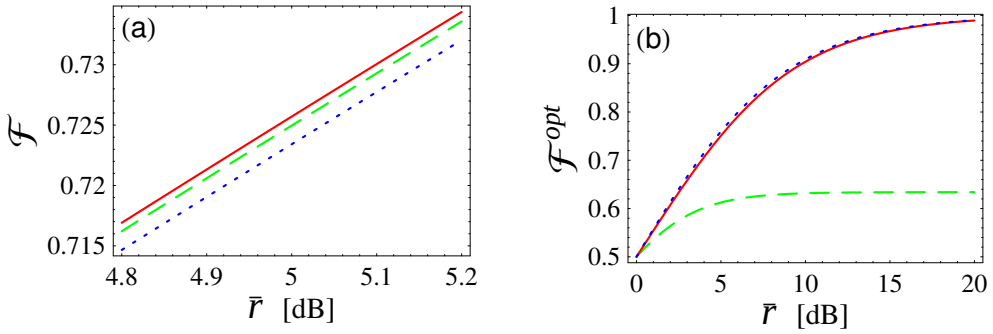

Figure 6. (a) Plot of the fidelities for teleporting an arbitrary coherent state from any sender to any receiver chosen from $N = 3$ parties, sharing a GHZ/W state. In a small window of average squeezing, we compare the optimal fidelity [41] (solid line), the fidelity obtained for the unbiased states discussed in Ref. [58] (dashed line), and the fidelity for states produced with all equal squeezers [39] (dotted line). The three curves are very close to each other, but the optimal preparation yields always the highest fidelity, as first proven in [41]. (b) Expected success for an experimental test of the promiscuous sharing of CV entanglement in GHZ/W states. Referring to the check-list in Sec. 6.1.2: the solid curve realizes point (i), being the optimal fidelity $\mathcal{F}_3^{opt}$ of a three-party teleportation network; the dotted curve realizes point (ii), being the optimal fidelity $\mathcal{F}_{2:uni}^{opt}$ of two-party teleportation exploiting the two-mode pure resource obtained from a unitary localization applied on two of the modes; the dashed curve realizes point (iii), being the optimal fidelity $\mathcal{F}_{2:red}^{opt}$ of two-party teleportation exploiting the two-mode mixed resource obtained discarding a mode. All of them lie above the classical threshold $\mathcal{F}^{cl} = 0.5$, providing a direct evidence of the promiscuity of entanglement sharing in the employed resources.

To detect the presence of tripartite entanglement, one should be able to implement the network in at least two different combinations [53], so that the teleportation would be accomplished, for instance, from mode 1 to mode 2 with the assistance of mode 3, and from mode 2 to mode 3 with the assistance of mode 1. To be complete (even if it is not strictly needed [15]), one could also realize the transfer from mode 3 to mode 1 with the assistance of mode 2. Taking into account a realistic asymmetry among the modes, the minimum experimental fidelity $\mathcal{F}_3^{opt}$ over the three possible situations would provide a direct quantitative measure of tripartite entanglement, through Eqs. (49–50).

To demonstrate the promiscuous sharing, one would then need to discard each one of the modes at a time, and perform standard two-user teleportation between the remaining pair of parties. The optimal fidelity for this two-user teleportation (which is achieved exactly for $r_1 = r_2 \equiv \bar{r}$) is

$$\mathcal{F}_{2:red}^{opt} = \frac{3}{3 + \sqrt{3 + 6e^{-4\bar{r}}}} \,. \tag{51}$$

Again, one should implement the three possible configurations and take the minimum fidelity as figure of merit. As anticipated in 6.1.2, this fidelity cannot reach unity because the entanglement in the shared mixed resource remains finite, and in fact $\mathcal{F}_{2:red}^{opt}$ saturates to $3/(3+\sqrt{3}) \approx 0.634$ in the limit of infinite squeezing.

Finding simultaneously both $\mathcal{F}_3^{opt}$ and $\mathcal{F}_{2:red}^{opt}$ above the classical threshold Eq. (47), at fixed squeezing $\bar{r}$, would be a clear experimental fingerprint of the promiscuous sharing of CV entanglement. Theoretically, this is true for all $\bar{r} > 0$, as shown in Fig. 6(b). From an experimental point of view, the tripartite teleportation network has been recently implemented, and the genuine tripartite shared entanglement unambiguosly demonstrated by

obtaining a nonclassical teleportation fidelity (up to 0.64 ± 0.02) in all the three possible user configurations [53]. Nevertheless, a nonclassical fidelity $\mathcal{F}_{2:red}$ in the teleportation exploiting any two-mode reduction was not observed.

This fact can be consistently explained by taking into account experimental noise. In fact, even if the desired resource states were pure GHZ/W states, the unavoidable effects of decoherence and imperfections resulted in the experimental production of *mixed* states, namely of the noisy GHZ/W states discussed in Sec. 3.1. It is very likely that the noise was too high compared with the pumped squeezing, so that the actual produced states were still fully inseparable, but laid outside the region of promiscuous sharing (see Fig. 1), having no entanglement left in the two-mode reductions. However, increasing the degree of initial squeezing, and/or reducing the noise sources might be accomplished with the state-of-the-art equipment employed in the experiments of Ref. [53] (see also [49]). The conditions required for a proper test (to be followed by actual practical applications) of the promiscuous sharing of CV entanglement in symmetric three-mode Gaussian states, as detailed in Sec. 6.1.2, should be thus met shortly. As a final remark, let us observe that repeating the same experiment but employing T states, described in Sec. 4.2, as resources, would be another interesting option. In fact, in this case the expected optimal fidelity is strictly smaller than in the case of GHZ/W states, confirming the promiscuous structure in which the reduced bipartite entanglement enhances the value of the genuine tripartite one.

With the same GHZ/W shared resources (but also with all symmetric and bisymmetric three-mode Gaussian states, including T states [2], noisy GHZ/W states and basset hound states), one may also test the power of the unitary localization of entanglement [9] (see Fig. 2), as opposed to the nonunitary localization of entanglement by measurements [59, 60], needed for the teleportation network. Suppose that the three parties Alice, Bob and Claire share a GHZ/W state. If Bob and Claire are allowed to cooperate (nonlocally), they can combine their respective modes at a 50:50 beam-splitter. The result is an entangled state shared by Alice and Bob, while Claire is left with an uncorrelated state. The optimal fidelity of standard teleportation from Alice to Bob with the unitarily localized resource, reads

$$\mathcal{F}_{2:uni}^{opt} = \left[\frac{1}{3}\left(\sqrt{4\cosh(4\bar{r})+5} - 2\sqrt{\cosh(4\bar{r})-1}\right)+1\right]^{-1}. \qquad (52)$$

Notice that $\mathcal{F}_{2:uni}$ is larger than $\mathcal{F}_3^{opt}$ [see Fig. 6(b)]. This is true for any number N of modes, and the difference between the two, at fixed squeezing, increases with N, confirming that the unitarily localizable entanglement of [9] is strictly stronger than the (nonunitarily) localizable entanglement of Refs. [59, 60], as discussed in Ref. [61]. This is of course not surprising, as the unitary localization generally requires a high degree of nonlocal control on the two subset of modes, while the localizable entangement is defined in terms of LOCC alone.

6.2. Degradation of teleportation efficiency under quantum noise

In Ref. [2] we have addressed the decay of three-partite entanglement (as quantified by the residual Gaussian contangle) of three-mode states in the presence of losses and thermal noise. We aim now at relating such an 'abstract' analysis to precise operational statements, by investigating the decay of the optimal teleportation fidelity of shared three-mode resources subject to environmental decoherence. This study will also provide further heuristic justification for the residual contangle as a proper measure of tripartite entanglement even for mixed ('decohered') Gaussian states. We will focus on the decay of the teleportation efficiency under decoherence affecting the resource states *after* their distribution to the distant parties.

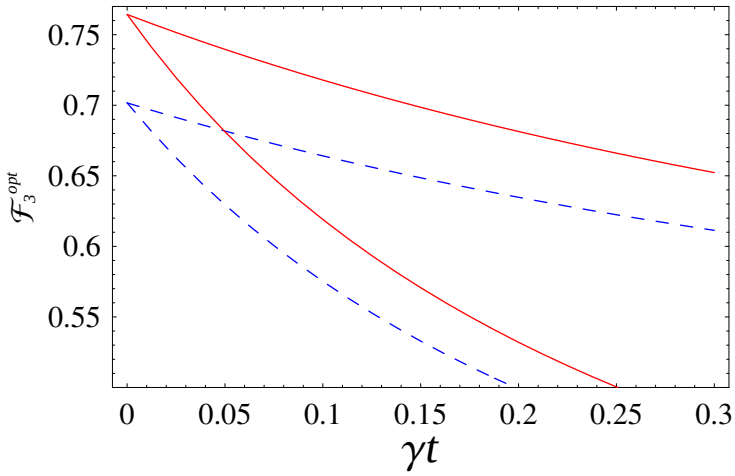

Figure 7. Evolution of the optimal fidelity $\mathcal{F}_3^{opt}$ for GHZ/W states with local mixedness $a = 2$ (corresponding to $\bar{r} \simeq 0.6842$) (solid curves) and T states with local mixedness $a = 2.8014$ (dashed curves). Such states have equal initial residual contangle but allow for different initial fidelities. The uppermost curves refer to baths with $n = 0$ ('pure losses'), while the lowermost curves refer to baths with $n = 1$. T states affording for the same initial fidelity as the considered GHZ/W state were also considered, and found to degrade faster than the GHZ/W state.

We will assume, realistically, a local decoherence (*i.e.* with no correlated noises) for the three modes, in thermal baths with equal average photon number n. The evolving states maintain their Gaussian character under such evolution (for a detailed description of the master equation governing the system and of its Gaussian solutions, refer to [2]).

As initial resources, we have considered both pure GHZ/W states and mixed T states, as described in Sec. 4.2. The results, showing the exact evolution of the fidelity $\mathcal{F}_3^{opt}$ (optimized over local unitaries) of teleportation networks exploiting such initial states, are shown in Fig. 7. GHZ/W states, already introduced as "optimal" resources for teleportation networks, were also found to allow for protocols most robust under decoherence. Notice how the qualitative behaviour of the curves of Fig. 7 follow that of Fig. 5 of Ref. [2], where the evolution of the residual Gaussian contangle of the same states under the same conditions is plotted. Also the vanishing of entanglement at finite times (occurring only in the presence of thermal photons, *i.e.* for $n > 0$) reciprocates the fall of the fidelity below the classical threshold of $1/2$. The status of the residual Gaussian contangle as a measure reflecting operational aspects of the states is thus strengthened in this respect, even in the region of mixed states. Notice, though, that Fig. 7 also shows that the entanglement of teleportation is *not* in general quantitatively equivalent (but for the pure-state case) to the residual Gaussian contangle, as the initial GHZ/W and T states of Fig. 7 have the same initial residual Gaussian contangle but grant manifestly different fidelities and, further, the times at which the classical threshold is trespassed do not exactly coincide with the times at which the residual contangle vanishes.

This confirms the special role of pure fully symmetric GHZ/W Gaussian states in tripartite CV quantum information, and the "uniqueness" of their entanglement under manifold interpretations as discussed in Sec. 6.1.2, much on the same footage as the "uniqueness" of entanglement in symmetric (mixed) two-mode Gaussian states (see Sec. 7.1)

Entanglement and optimal fidelity for nonsymmetric Gaussian resources?

Throughout this whole section, we have only dealt with completely symmetric resource states, due to the invariance requirements of the considered protocol. In Ref. [41], the question whether expressions like Eq. (49), connecting the optimal teleportation fidelity to the entanglement in the shared resource, were valid as well for nonsymmetric entangled resource states, was left open (see also Ref. [45]). In Sec. 7, devoted to telecloning, we will show with a specific counterexample that this is *not* the case, not even in the simplest case of $N = 2$.

7. $1 \rightarrow 2$ telecloning with bisymmetric and nonsymmetric resources

Quantum *telecloning* [62] among $N + 1$ parties is defined as a process in which one party (Alice) owns an unknown quantum state, and wants to distribute her state, via teleportation, to all the other N remote parties. The no-cloning theorem [63, 64] yields that the N remote clones can resemble the original input state only with a finite, nonmaximal fidelity. In CV systems, $1 \rightarrow N$ telecloning of arbitrary coherent states was proposed in Ref. [31], involving a special class of $(N + 1)$-mode multiparty entangled Gaussian states (known as "multiuser quantum channels") shared as resources among the $N + 1$ users. The telecloning is then realized by a succession of standard two-party teleportations between the sender Alice and each of the N remote receivers, exploiting each time the corresponding reduced two-mode state shared by the selected pair of parties.

Depending on the symmetries of the shared resource, the telecloning can be realized with equal fidelities for all receivers (*symmetric* telecloning) or with unbalanced fidelities among the different receivers (*asymmetric* telecloning). In particular, in the first case, the needed resource must have complete invariance under mode permutations in the N-mode block distributed among the receivers: the resource state has to be thus a $1 \times N$ bisymmetric state [10, 9] (see Fig. 2).

In this manuscript we specialize on $1 \rightarrow 2$ telecloning, where Alice, Bob and Claire share a tripartite entangled three-mode Gaussian state and Alice wants to teleport arbitrary coherent states to Bob and Claire with certain fidelities. As the process itself suggests, the crucial resource enabling telecloning is not the genuine tripartite entanglement (needed instead for a successful 'multidirectional' teleportation network, as shown in the previous section), but the couplewise entanglement between the pair of modes $1|2$ and $1|3$ [if the sender (Alice) owns mode 1, while the receivers (Bob and Claire) own modes 2 and 3].

Let us notice that, very recently, the first experimental demonstration of unconditional symmetric $1 \rightarrow 2$ telecloning of unknown coherent states has been achieved by Furusawa's group [65], with a fidelity for each clone of $\mathcal{F} = 0.58 \pm 0.01$, surpassing the classical threshold of 0.5, Eq. (47). This experimental milestone has raised renewed interest towards CV quantum communication [66]. Moreover, in keep with the general spirit of the paper, the context of CV telecloning constitutes here the proper testground to investigate the operational significance of the proposed entanglement measures. The present analysis will lead to conclusively show that the correspondence between entanglement and teleportation fidelity does not extend to non-symmetric Gaussian states.

7.1. Symmetric telecloning

Let us first analyze the case of symmetric telecloning, occurring when Alice aims at sending two copies of the original state with equal fidelities to Bob and Claire. In this case it has been

proven [67, 68, 31] that Alice can teleport an arbitrary coherent state to the two distant twins Bob and Claire (employing a Gaussian cloning machine) with the maximal fidelity

$$\mathcal{F}_{\max}^{1\to 2} = \frac{2}{3}\,. \tag{53}$$

This argument inspired the introduction of the 'no-cloning threshold' for two-party teleportation [69], basically stating that only a fidelity greater than $2/3$ (thus greater than the previously introduced threshold of $1/2$, which implies the presence of entanglement) ensures the realization of actual two-party quantum teleportation of a coherent state. In fact, if the fidelity falls in the range $1/2 < \mathcal{F} < 2/3$, then Alice could have kept a better copy of the input state for herself, or sent it to a 'malicious' Claire. In this latter case, the whole process would result into an asymmetric telecloning, with a fidelity $\mathcal{F} > 2/3$ for the copy received by Claire. It is worth remarking that, as already mentioned, two-party CV teleportation beyond the no-cloning threshold has been also recently demonstrated experimentally, with a fidelity $\mathcal{F} = 0.70 \pm 0.02$ [49]. Another important and surprising remark is that the fidelity of $1 \to 2$ cloning of coherent states, given by Eq. (53), is *not* the optimal one. As recently shown in Ref. [70], using non-Gaussian operations as well, two identical copies of an arbitrary coherent state can be obtained with optimal single-clone fidelity $\mathcal{F} \approx 0.6826$.

In our setting, dealing with Gaussian states and Gaussian operations only, Eq. (53) represents the maximum achievable success for symmetric $1 \to 2$ telecloning of coherent states. As previously anticipated, the *basset hound states* $\boldsymbol{\sigma}_B^p$ of Sec. 3.2 are the best suited resource states for this task. Such states belong to the family of multiuser quantum channels introduced in Ref. [31], and are 1×2 bisymmetric pure states, parametrized by the single-mode mixedness a of mode 1. In particular, it is interesting to study how the single-clone telecloning fidelity behaves compared with the actual amount of entanglement in the $1|l$ ($l = 2, 3$) nonsymmetric two-mode reductions of $\boldsymbol{\sigma}_B^p$ states.

A brief excursus has to be made here. Setting, as usual, all first moments to zero, the fidelity of two-user teleportation of arbitrary single-mode Gaussian states exploiting two-mode Gaussian resources can be computed directly from the respective CMs [71]. Being $\boldsymbol{\sigma}_{in}$ the CM of the unknown input state, and

$$\boldsymbol{\sigma}_{ab} = \begin{pmatrix} \boldsymbol{\sigma}_a & \boldsymbol{\varepsilon}_{ab} \\ \boldsymbol{\varepsilon}_{ab}^{\mathsf{T}} & \boldsymbol{\sigma}_b \end{pmatrix}\,, \tag{54}$$

the CM of the shared two-mode resource, and defining the matrix $\boldsymbol{\xi} = \mathrm{diag}\{-1\,, 1\}$, the fidelity reads [71]

$$\mathcal{F} = \frac{2}{\sqrt{\mathrm{Det}\,\boldsymbol{\Sigma}}}\,, \qquad \boldsymbol{\Sigma} \equiv 2\,\boldsymbol{\sigma}_{in} + \boldsymbol{\xi}\boldsymbol{\sigma}_a\boldsymbol{\xi} + \boldsymbol{\sigma}_b + \boldsymbol{\xi}\boldsymbol{\varepsilon}_{ab} + \boldsymbol{\varepsilon}_{ab}^{\mathsf{T}}\boldsymbol{\xi}\,. \tag{55}$$

In our case, $\boldsymbol{\sigma}_{in} = \mathbb{1}_2$ because Alice is teleporting coherent states, while the resource $\boldsymbol{\sigma}_{ab}$ is obtained discarding either the third ($a = 1$, $b = 2$) or the second ($a = 1$, $b = 3$) mode from the CM $\boldsymbol{\sigma}_B^p$ of basset hound states. From Eqs. (16, 17, 55), the single-clone fidelity for symmetric $1 \to 2$ telecloning exploiting basset hound states is:

$$\mathcal{F}_{sym}^{1\to 2} = \frac{4}{3a - 2\sqrt{2}\sqrt{a^2-1} + 5}\,. \tag{56}$$

Notice, remembering that each of modes 2 and 3 contains an average number of photons $\bar{n} = (a-1)/2$, that Eq. (56) is the same as Eq. (19) of Ref. [72], where a production scheme for three-mode Gaussian states by interlinked nonlinear interactions in $\chi^{(2)}$ media is presented, and the usefulness of the produced resources for $1 \to 2$ telecloning is discussed as well. The basset hound states realize an optimal symmetric cloning machine, *i.e.* the fidelity of both clones saturates Eq. (53), for the finite value $a = 3$. Surprisingly, with increasing

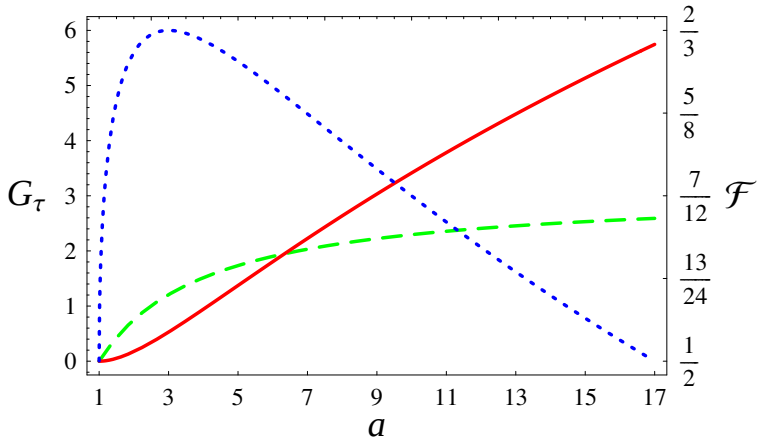

Figure 8. Bipartite entanglement $G_\tau^{1|l}$ (dashed line) in $1|l$ ($l = 2, 3$) two-mode reductions of basset hound states, and genuine tripartite entanglement G_τ^{res} (solid line) among the three modes, versus the local mixedness a of mode 1. Entanglements are quantified by the Gaussian contangle. The fidelity $\mathcal{F}_{sym}^{1\to 2}$ of symmetric $1 \to 2$ telecloning employing basset hound resource states is plotted as well (dotted line, scaled on the right axis), reaching its optimal value of $2/3$ for $a = 3$.

$a > 3$, the fidelity Eq. (56) starts decreasing, even if the two-mode entanglements Eq. (20) in the reduced (nonsymmetric) bipartitions of modes $1|2$ and $1|3$, as well as the genuine tripartite entanglement Eq. (18), increase with increasing a. As shown in Fig. 8, the telecloning fidelity is not a monotonic function of the employed bipartite entanglement. Rather, it roughly follows the difference $G_\tau^{1|l} - G_\tau^{res}$, being maximized where the bipartite entanglement is stronger than the tripartite one. This fact heuristically confirms that in basset hound states bipartite and tripartite entanglements are competitors, meaning that the CV entanglement sharing in these states is not promiscuous, as described in Sec. 3.2.

The example of basset hound states represents a clear hint that the teleportation fidelity with general two-mode (pure or mixed) nonsymmetric resources is *not* monotone with the entanglement. Even if an hypothetical optimization of the fidelity over the local unitary operations could be performed (on the guidelines of [41]), it would entail a fidelity growing up to $2/3$ and then staying constant while entanglement increases, which means that no direct estimation of the entanglement can be extracted from the nonsymmetric teleportation fidelity, at variance with the symmetric case (see the previous section). More precisely, it can be easily shown that the direct relationship between negativity and teleportation fidelity valid for symmetric states cannot carry over to nonsymmetric resources as well. In point of fact, applying it to the $1|l$ ($l = 2, 3$) two-mode reduced resources obtained from basset hound states, would imply an "optimal" fidelity reaching $3/4$ in the limit $a \to \infty$. But this value is impossible to achieve, even considering non-Gaussian cloning machines [70]: thus, the simple relation between teleportation fidelity and entanglement, formalized by Eq. (49), fails to hold for nonsymmetric resources, even in the basic two-mode instance. Let us mention that the relationship between entanglement and teleportation fidelity had already been partially addressed in Ref. [73] (which also points out other counterintuitive features occurring for asymmetric mixed resources, like the enhancement of fidelity under suitable noisy pre-processing). However, Ref. [73] actually addresses the relationship between teleportation

fidelity and the squeezing parameter of an asymmetrically decohered two-mode squeezed state (used as the entangled resource). We remark that such a quantity, while being related to the entanglement of the state is not, by itself, a proper entanglement quantifier (*e.g.*, it does not determine the negativity of the nonsymmetric state).

This somewhat controversial result can be to some extent interpreted as follows. For symmetric Gaussian states, there exists a 'unique type' of bipartite CV entanglement. In fact, measures such as the logarithmic negativity (quantifying the violation of the mathematical PPT criterion), the entanglement of formation (related to the entanglement cost, and thus quantifying how expensive is the process of creating a mixed entangled state through LOCC), and the degree of EPR correlation (quantifying the correlations between the entangled degrees of freedom) are *all* completely equivalent for such states, being monotonic functions of only the smallest symplectic eigenvalue $\tilde{\nu}_-$ of the partially transposed CM. As we have seen, this equivalence extends also to the efficiency of two-user quantum teleportation, quantified by the fidelity optimized over local unitaries. For nonsymmetric states, the chain of equivalences breaks down. In hindsight, this could have been somehow expected, as there exist several inequivalent but legitimate measures of entanglement, each of them capturing distinct aspects of the quantum correlations (one could think, for instance, of the operative difference existing between the definitions of distillable entanglement and entanglement cost). In the specific instance of nonsymmetric two-mode Gaussian states, it has been shown that the negativity is neither equivalent to the (Gaussian) entanglement of formation (the two measures may induce inverted orderings on this subset of entangled states) [74], nor to the EPR correlation [75]. It is thus justified that a process like teleportation emphasizes a distinct aspect of the entanglement encoded in nonsymmetric resources. Notice also that the richer and more complex entanglement structure of non symmetric states, as compared to that of symmetric states, reflects a crucial operational difference in the respective (asymmetric and symmetric) teleportation protocols. While in the symmetric protocols the choice of sender and receiver obviously does not affect the fidelity, this is no longer the case in the asymmetric instance: this physical asymmetry between sender and receiver properly exemplifies the more complex nature of the two-mode asymmetric entanglement.

7.2. Asymmetric telecloning

In this section we focus on the *asymmetric* telecloning of coherent states, through generic pure three-mode Gaussian states shared as resources among the three parties. Considering states in standard form (see Sec. 4.1 and Ref. [2]), parametrized by the local single-mode mixednesses a_i of modes $i = 1, 2, 3$, the fidelity $\mathcal{F}^{1\to 2}_{asym:2}$ of Bob's clone (employing the $1|2$ two-mode reduced resource) can be computed from Eq. (55) and reads

$$\mathcal{F}^{1\to 2}_{asym:2} = 2\left\{ -2a_3^2 + 2a_1a_2 + 4\,(a_1+a_2) + 3\left(a_1^2+a_2^2\right) \right. \tag{57}$$
$$\left. -\ (a_1+a_2+2)\sqrt{\frac{[(a_1+a_2-a_3)^2-1][(a_1+a_2+a_3)^2-1]}{a_1a_2}} + 2 \right\}^{-\frac{1}{2}},$$

Similarly, the fidelity $\mathcal{F}^{1\to 2}_{asym:3}$ of Claire's clone can be obtained from Eq. (57) by exchanging the roles of "2" and "3".

It is interesting to explore the space of parameters $\{a_1,\, a_2,\, a_3\}$ in order to find out which three-mode states allow for an asymmetric telecloning with the fidelity of one clone above the symmetric threshold of $2/3$, while keeping the fidelity of the other clone above the classical threshold of $1/2$. Let us keep a_1 fixed. With increasing difference between a_2 and a_3, one of

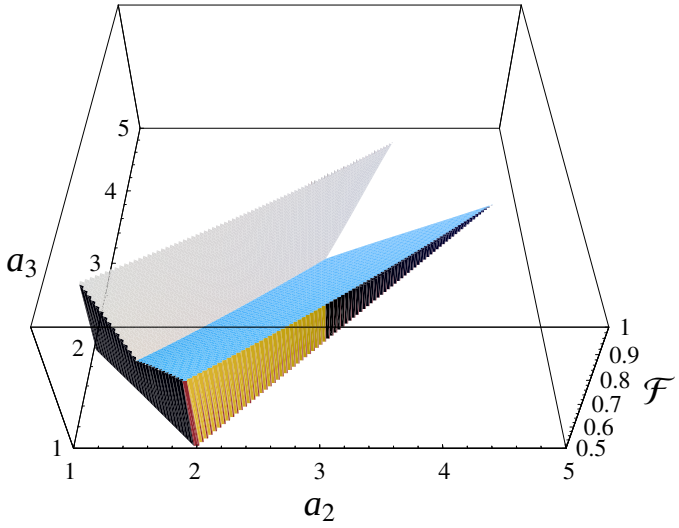

Figure 9. Fidelities for asymmetric telecloning with three-mode pure Gaussian resources, at a fixed $a_1 = 2$, as functions of a_2 and a_3, varying in the allowed range of parameters constrained by Ineq. (6) (see also Fig. 4). The darker surface on the right-hand side of the diagonal $a_2 = a_3$ (along which the two surfaces intersect) is the fidelity of Bob's clone, $\mathcal{F}^{1\to 2}_{asym:2}$, while the lighter, 'mirror-reflected' surface on the left-hand side of the diagonal is the fidelity of Claire's clone, $\mathcal{F}^{1\to 2}_{asym:3}$. Only nonclassical fidelities (*i.e.* $\mathcal{F} > 1/2$) are shown.

the two telecloning fidelities increases at the detriment of the other, while with increasing sum $a_2 + a_3$ both fidelities decrease to fall eventually below the classical threshold, as shown in Fig. 9. The asymmetric telecloning is thus *optimal* when the sum of the two local mixednesses of modes 2 and 3 saturates its lower bound. From Ineq. (6), the optimal resources must have

$$a_3 = a_1 - a_2 + 1\,, \tag{58}$$

A suitable parametrization of these states is obtained setting $a_1 \equiv a$ and

$$a_2 = 1 + (a-1)t\,, \qquad 0 \le t \le 1\,. \tag{59}$$

For $t < 1/2$ the fidelity of Bob's clone is smaller than that of Claire's one, $\mathcal{F}^{1\to 2}_{asym:2} < \mathcal{F}^{1\to 2}_{asym:3}$, while for $t > 1/2$ the situation is reversed. In all the subsequent discussion, notice that Bob and Claire swap their roles if t is replaced by $1 - t$. For $t = 1/2$, the asymmetric resources reduce to the bisymmetric basset hound states useful for symmetric telecloning. The optimal telecloning fidelities then read

$$\mathcal{F}^{opt:1\to 2}_{asym:2} = \frac{2}{\sqrt{(a+3)^2+(a-1)^2t^2+2(a-1)(3a+5)t-4\sqrt{(a^2-1)t}[a+(a-1)t+3]}}\,, \tag{60}$$

and similarly for $\mathcal{F}^{opt:1\to 2}_{asym:3}$ replacing t by $1 - t$. The two optimal fidelities are plotted in Fig. 10

With these pure nonsymmetric resources, further optimizations can be performed depending on the needed task. For instance, one may need to implement telecloning with the highest possible fidelity of one clone, while keeping the other nonclassical. This problem is of straightforward solution, and yields optimal asymmetric resources with

$$a = \frac{7}{2}\,, \quad t = \frac{4}{5}\,. \tag{61}$$

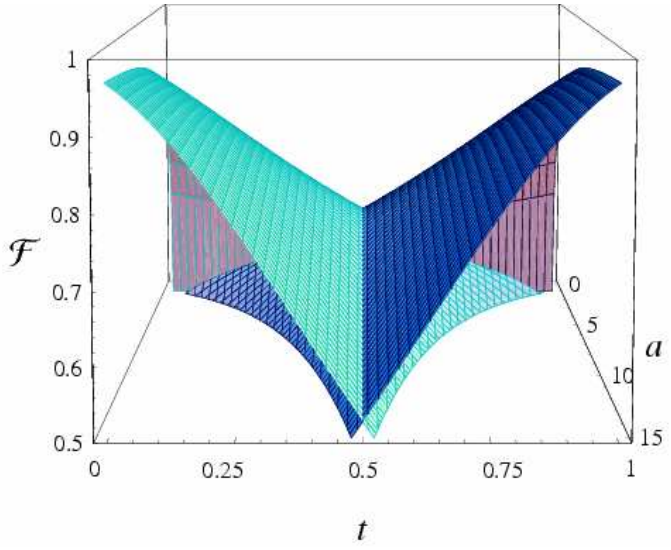

Figure 10. Optimal fidelities for asymmetric telecloning with three-mode pure Gaussian resources, as functions of the single-mode mixedness a of mode 1, and of the parameter t determining the local mixednesses of the other modes, through Eqs. (58,59). The darker, rightmost surface is the optimal fidelity of Bob's clone, $\mathcal{F}_{asym:2}^{opt:1\to 2}$, while the lighter, leftmost surface is the optimal fidelity of Claire's clone, $\mathcal{F}_{asym:3}^{opt:1\to 2}$. Along the intersection line $t = 1/2$ the telecloning is symmetric. Only nonclassical fidelities (*i.e.* $\mathcal{F} > 1/2$) are shown.

In this case the fidelity of Claire's clone saturates the classical threshold, $\mathcal{F}_{asym:3}^{opt:1\to 2} = 1/2$, while the fidelity of Bob's clone reaches $\mathcal{F}_{asym:3}^{opt:1\to 2} = 4/5$, which is the maximum allowed value for this setting [76]. Also, choosing $t = 1/5$, Bob's fidelity gets classical and Claire's fidelity is maximal.

In general, a telecloning with $\mathcal{F}_{asym:2}^{opt:1\to 2} \geq 2/3$ and $\mathcal{F}_{asym:3}^{opt:1\to 2} \geq 1/2$ is possible only in the window

$$1.26 \approx 2\sqrt{2}\left[2 - \sqrt{1+\sqrt{2}}\right] \leq a \leq 2\sqrt{2}\left[2 + \sqrt{1+\sqrt{2}}\right] \approx 10.05 \quad (62)$$

and, for each a falling in the region defined by Ineq. (62), in the specific range

$$\frac{a - 2\sqrt{a+1} + 2}{a-1} \leq t \leq \frac{2\left(\sqrt{2}\sqrt{a+1} - 2\right)}{a-1}\,. \quad (63)$$

For instance, for $a = 3$, the optimal asymmetric telecloning (with Bob's fidelity above no-cloning and Claire's fidelity above classical bound) is possible in the whole range $1/2 \leq t \leq 2\sqrt{2} - 1$, where the boundary $t = 1/2$ denotes the basset hound state realizing optimal symmetric telecloning (see Fig. 8). The sum $\mathcal{S}^{opt:1\to 2} = \mathcal{F}_{asym:2}^{opt:1\to 2} + \mathcal{F}_{asym:3}^{opt:1\to 2}$ can be maximized as well, and the optimization is realized by values of a falling in the range $2.36 \lesssim a \leq 3$, depending on t. The absolute maximum of $\mathcal{S}^{opt:1\to 2}$ is reached, as expected, in the fully symmetric instance $t = 1/2$, $a = 3$, and yields $\mathcal{S}_{\max}^{opt:1\to 2} = 4/3$.

We finally recall that optimal three-mode Gaussian resources, can be produced by implementing the allotment operator (see Sec. 4.1), and employed to perform all-optical symmetric and asymmetric telecloning machines [31, 76].

8. Conclusions

In the present paper and in Ref. [2], we have aimed at providing a (to a good extent) comprehensive treatment on the characterization, quantification and experimental generation of genuine multipartite entanglement in three-mode Gaussian states of CV systems, including relevant, practical implementations in the context of CV quantum information.

Similarly with what happens for bipartite entanglement in symmetric Gaussian states, but at striking variance with the discrete-variable scenario (in particular for systems of three qubits), we have shown that there is a *unique* kind of genuine tripartite entanglement in pure, symmetric, three-mode Gaussian states, which combines a mathematical significance in the context of entanglement sharing with an operational interpretation in terms of teleportation experiments. This fact is a remarkable consequence of the restriction to Gaussian states, as the proven existence, for infinite dimensional systems, of infinitely many mutually stochastic-LOCC-incomparable states (even under the bounded energy and finite information exchange condition) suggests [77]. Even more strikingly, this tripartite entanglement distributes in a *promiscuous* way, being enhanced by the presence of bipartite entanglement in any two-mode reduction. Here we have shown that the promiscuity of CV entanglement survives even for non-pure states like noisy GHZ/W states, with purities down to 0.2. However, with increasing mixedness the structure of three-party entanglement enriches, as tripartite bound entangled states can exist even in the fully symmetric instance. For nonsymmetric (pure or mixed) three-mode states, the promiscuity fades leaving room for a more traditional entanglement sharing structure. We further remark that for all fully inseparable Gaussian states (which represent one of the five possible separability classes [1]), the residual Gaussian contangle, or *arravogliament*, is a *bona fide*, computable measure of genuine tripartite entanglement, as first demonstrated in Refs. [3, 2], and evaluated in several explicit instances here.

The core of this paper has been devoted to providing several examples of tripartite entangled Gaussian states, relevant for their entanglement properties and/or for applications in CV quantum information. For each of them, we have computed the tripartite entanglement explicitly, and dedicated great attention to quantum state engineering, proposing schemes for the experimental production of the considered states. In particular we developed a self-contained procedure to engineer (up to local operations) arbitrary pure three-mode Gaussian states by means of linear optics, based on the distribution, or *allotment* of two-mode entanglement among three modes.

In the last part of this work we have investigated the potentialities of the introduced families of three-mode Gaussian states for the implementation of multipartite quantum communication protocols with continuous variables. This has allowed us to focus on the physical significance of the applied 'genuine multipartite' entanglement measure (arravogliament), shifting the analysis's testing ground from the domain of mathematical convenience to that of operational effectiveness.

Acknowledgments

Financial support from MIUR, INFN, and CNR is acknowledged. G A is grateful to Samanta Piano for her encouraging advice, and for reminding him of the sentence quoted in the caption of Fig. 2. A S is currently a Marie Curie fellow at Imperial College London; he also acknowledges EPSRC for financial support (through the QIP-IRC) and the Centre for Mathematical Sciences of the University of Cambridge for kind hospitality.

References

[1] Giedke G, Kraus B, Lewenstein M and Cirac J I 2001 *Phys. Rev. A* **64** 052313
[2] Adesso G, Serafini A and Illuminati F 2006 *Phys. Rev. A* **73** 032345
[3] Adesso G and Illuminati F 2006 *New J. Phys.* **8** 15
[4] Braunstein S L and Pati A K (eds) 2003 *Quantum Information Theory with Continuous Variables* (Dordrecht: Kluwer Academic Publishers)
[5] Cerf N, Leuchs G and Polzik E S (eds) 2007 in press *Quantum Information with Continuous Variables of Atoms and Light* (London: Imperial College Press)
[6] Braunstein S L and van Loock P 2005 *Rev. Mod. Phys.* **77** 513
[7] Adesso G and Illuminati F 2007 *Preprint* quant-ph/0701221; Adesso G *PhD Thesis* (Università degli Studi di Salerno, 2007) available as *Preprint* quant-ph/0702069
[8] Simon R, Sudarshan E C G and Mukunda N 1987 *Phys. Rev. A* **36** 3868
[9] Serafini A, Adesso G and Illuminati F 2005 *Phys. Rev. A* **71** 032349
[10] Adesso G, Serafini A and Illuminati F 2004 *Phys. Rev. Lett.* **93** 220504
[11] Simon R 2000 *Phys. Rev. Lett.* **84** 2726
[12] Duan L-M, Giedke G, Cirac J I and Zoller P 2000 *Phys. Rev. Lett.* **84** 2722
[13] Werner R F and Wolf M M 2001 *Phys. Rev. Lett.* **86** 3658
[14] Vidal G and Werner R F 2002 *Phys. Rev. A* **65** 032314
[15] van Loock P and Furusawa A 2003 *Phys. Rev. A* **67** 052315
[16] Hyllus P and Eisert J 2006 *New J. Phys.* **8** 51
[17] Hiroshima T, Adesso G and Illuminati F 2007 *Phys. Rev. Lett.* **98** 050503
[18] Adesso G and Illuminati F 2006 *Int. J. Quant. Inf* **4** 383
[19] Coffman V, Kundu J and Wootters W K 2000 *Phys. Rev. A* **61** 052306
[20] Osborne T J and Verstraete F 2006 *Phys. Rev. Lett.* **96** 220503
[21] Paris M G A, Illuminati F, Serafini A and De Siena S 2003 *Phys. Rev. A* **68** 012314
[22] Dür W, Vidal G and Cirac J I 2000 *Phys. Rev. A* **62** 062314
[23] Adesso G, Ericsson M and Illuminati F 2006 *Preprint* quant-ph/0609178
[24] Chen X-Y 2005 *Phys. Lett. A* **335** 121
[25] Pirandola S, Mancini S, Vitali D and Tombesi P 2003 *Phys. Rev. A* **68** 062317
[26] Ferraro A and Paris M G A 2005 *Phys. Rev. A* **72** 032312
[27] Illuminati F 2001 public lecture. NO ANIMALS WERE HARMED IN THE MAKING OF FIGURE 2.
[28] Holevo A S and Werner R F 2001 *Phys. Rev. A* **63** 032312
[29] Botero A and Reznik B 2003 *Phys. Rev. A* **67** 052311
[30] Giedke G, Eisert J, Cirac J I and Plenio M B 2003 *Quant. Inf. Comp.* **3** 211
[31] van Loock P and Braunstein S L 2001 *Phys. Rev. Lett.* **87** 247901
[32] Wolf M M, Verstraete F and Cirac J I 2004 *Phys. Rev. Lett.* **92** 087903
[33] Aoki T, Takei N, Yonezawa H, Wakui K, Hiraoka T, Furusawa A and van Loock P 2003 *Phys. Rev. Lett.* **91** 080404
[34] Bradley A S, Olsen M K, Pfister O and Pooser R C 2005 *Phys. Rev. A* **72** 053805
[35] For a review on quantum optical state engineering see Dell'Anno F, De Siena S and Illuminati F 2006 *Phys. Rep.* **428** 53
[36] Arvind, Dutta B, Mukunda N and Simon R 1995 *Pramana* **45** 471, available as *Preprint* quant-ph/9509002
[37] Adesso G 2006 *Phys. Rev. Lett.* **97** 130502
[38] Laurat J, Keller G, Oliveira-Huguenin J A, Fabre C, Coudreau T, Serafini A, Adesso G and Illuminati F 2005 *J. Opt. B* **7** S577
[39] van Loock P and Braunstein S L 2000 *Phys. Rev. Lett.* **84** 3482
[40] Braunstein S L 1998 *Nature* **394** 47
[41] Adesso G and Illuminati F 2005 *Phys. Rev. Lett.* **95** 150503
[42] Bennett C H, Brassard G, Crépeau C, Jozsa R, Peres A and Wootters W K 1993 *Phys. Rev. Lett.* **70** 1895
[43] Bouwmeester D, Pan J-W, Mattle K, Eibl M, Weinfurter H and Zeilinger A 1997 *Nature* **390** 575
[44] Boschi D, Branca S, De Martini F, Hardy L and Popescu S 1998 *Phys. Rev. Lett.* **80** 1121
[45] Pirandola S and Mancini S 2006 *Laser Physics* **16** 1418
[46] Vaidman L 1994 *Phys. Rev. A* **49** 1473
[47] Braunstein S L and Kimble H J 1998 *Phys. Rev. Lett.* **80** 869
[48] Furusawa A, Sørensen J L, Braunstein S L, Fuchs C A, Kimble H J and Polzik E S 1998 *Science* **282** 706 (1998)
[49] Takei N, Yonezawa H, Aoki T and Furusawa A 2005 *Phys. Rev. Lett.* **94** 220502
[50] Braunstein S L, Fuchs C A and Kimble H J 2000 *J. Mod. Opt.* **47** 267
[51] Hammerer K, Wolf M M, Polzik E S and Cirac J I 2005 *Phys. Rev. Lett.* **94** 150503
[52] Pirandola S 2005 *Int. J. Quant. Inf.* **3** 239
[53] Yonezawa H, Aoki T and Furusawa A 2004 *Nature* **431** 430

[54] Pirandola S and Mancini S and Vitali D 2005 *Phys. Rev. A* **71** 042326; erratum *ibid.* **72** 059901
[55] Lance A M, Symul T, Bowen W P, Sanders B C and Lam P K 2004 *Phys. Rev. Lett.* **92** 177903
[56] Jing J, Zhang J, Yan Y, Zhao F, Xie C and Peng K 2003 *Phys. Rev. Lett.* **90** 167903
[57] Neigovzen R and Sanpera A 2005 *Preprint* quant-ph/0507249
[58] Bowen W P, Lam P K and Ralph T C 2003 *J. Mod. Opt.* **50** 801
[59] Verstraete F, Popp M, and Cirac J I 2004 *Phys. Rev. Lett.* **92** 027901
[60] Popp M, Verstraete F, Martin-Delgado M A and Cirac J I 2005 *Phys. Rev. A* **71** 042306
[61] Adesso G and Illuminati F *Bipartite and Multipartite Entanglement of Gaussian States* in [5], available as *Preprint* quant-ph/0510052
[62] Murao M, Jonathan D, Plenio M B and Vedral V 1999 *Phys. Rev. A* **59** 156
[63] Wootters W K and Zurek W H 1982 *Nature* **299** 802
[64] Dieks D 1982 *Phys. Lett. A* **92** 271
[65] Koike S, Takahashi H, Yonezawa H, Takei N, Braunstein S L, Aoki T and Furusawa A 2006 *Phys. Rev. Lett.* **96** 060504
[66] See *e.g.* some press coverage on the telecloning experiment [65]:
`http://www.newscientist.com/channel/fundamentals/dn8756.html`,
`http://www.aip.org/pnu/2006/split/765-1.html`,
`http://physicsweb.org/articles/news/10/2/15/1`,
and The Japan Journal, September 2006 issue, page 30-31
[67] Cerf N J, Ipe A and Rottenberg X 2000 *Phys. Rev. Lett.* **85** 1754
[68] Cerf N J and Iblisdir S 2000 *Phys. Rev. A* **62** 040301(R)
[69] Grosshans F and Grangier P 2001 *Phys. Rev. A* **64** 010301(R)
[70] Cerf N J, Krüger O, Navez P, Werner R F and Wolf M M 2005 *Phys. Rev. Lett.* **95** 070501
[71] Fiurášek J 2002 *Phys. Rev. A* **66** 012304
[72] Ferraro A, Paris M G A, Allevi A, Andreoni A, Bondani M and Puddu E 2004 *J. Opt. Soc. Am. B* **21** 1241
[73] Kim M S and Lee J 2001 *Phys. Rev. A* **64** 012309
[74] Adesso G and Illuminati F 2005 *Phys. Rev. A* **72** 032334
[75] Adesso G, Serafini A and Illuminati F 2004 *Phys. Rev. A* **70** 022318
[76] Fiurášek J 2001 *Phys. Rev. Lett.* **86** 4942
[77] Owari M, Matsumoto K and Murao M 2004 *Phys. Rev. A* **70** 050301(R)